AD-A118 865 ANALYTICS INC BLOOMINGTON IN F/G 14/2
A MODEL OF EDDY-CURRENT PROBES WITH FERRITE CORES.(U)
APR 82 H A SABBAGH N60921-81-C-0076
UNCLASSIFIED TR-1-82 NL

END
DATE FILMED
10-82
DTIC

UNCLASSIFIED

SECURITY CLASSIFICATION OF THIS PAGE (When Data Entered)

REPORT DOCUMENTATION PAGE		READ INSTRUCTIONS BEFORE COMPLETING FORM
1. REPORT NUMBER TR1-82	2. GOVT ACCESSION NO. AD-A118865	3. RECIPIENT'S CATALOG NUMBER
4. TITLE (and Subtitle) A MODEL OF EDDY-CURRENT PROBES WITH FERRITE CORES		5. TYPE OF REPORT & PERIOD COVERED FINAL REPORT 6. PERFORMING ORG. REPORT NUMBER
7. AUTHOR(s) Harold A. Sabbagh		8. CONTRACT OR GRANT NUMBER(s) N60921-81-C-0076
9. PERFORMING ORGANIZATION NAME AND ADDRESS Analytics, Inc. 2634 Round Hill Lane Bloomington, IN 47401		10. PROGRAM ELEMENT, PROJECT, TASK AREA & WORK UNIT NUMBERS 62767N, WF61542, R34BA
11. CONTROLLING OFFICE NAME AND ADDRESS Naval Surface Weapons Center (Code R34) White Oak Labs Silver Spring, MD 20910		12. REPORT DATE 19 April 1982 13. NUMBER OF PAGES 55
14. MONITORING AGENCY NAME & ADDRESS(if different from Controlling Office)		15. SECURITY CLASS. (of this report) Unclassified 15a. DECLASSIFICATION/DOWNGRADING SCHEDULE

16. DISTRIBUTION STATEMENT (of this Report)

Distribution Unlimited: Approved for Public Release

17. DISTRIBUTION STATEMENT (of the abstract entered in Block 20, if different from Report)

18. SUPPLEMENTARY NOTES

19. KEY WORDS (Continue on reverse side if necessary and identify by block number)

Eddy-currents
Nondestructive evaluation
Numerical electromagnetic modeling
Method of moments
Volume integral equation

20. ABSTRACT (Continue on reverse side if necessary and identify by block number)

We develop a model of a three-dimensional axisymmetric probe coil with a ferrite core in the presence of a conducting half-space (the workpiece). The half-space is accounted for by computing the appropriate Green's function by using Bessel transforms. Upon introducing equivalent Amperian currents within the core, we derive a volume integral equation, whose unknown is either the magnetic induction field, or induced magnetization, and whose kernel is the Green's function that was previously derived. The integral

DD FORM 1 JAN 73 1473 EDITION OF 1 NOV 65 IS OBSOLETE
S/N 0102-LF-014-6601

SECURITY CLASSIFICATION OF THIS PAGE (When Data Entered)

(20) (cont)

equation is transformed, via the method of moments, into a vector-matrix equation, which is then solved using a linear equation solver. This allows us to compute the magnetic induction field within the core, the driving-point impedance of the coil/core combination, and the induced eddy-currents within the workpiece. Results of these calculations are presented; in addition, a brief description of extensions of the model to linear and nonlinear pulsed eddy-current problems, problems with anisotropic cores, and optimization of core shaping to provide specific eddy-current flow patterns is given.

I. INTRODUCTION

The classical work of Dodd and his coworkers at the Oak Ridge National Laboratory deals with the analysis, design and optimization of eddy-current proble coils wound around an air core. Many applications, however, require that the magnetic field produced by the probe coil be "shaped" or confined to certain regions of space, especially at higher frequencies, and this necessitates the use of highly permeable core materials, such as ferrites.

The problem we propose to solve is depicted in Figure 1. It consists of an arbitrarily shaped body-of-revolution made of a ferrite (or other highly permeable material), excited by a coaxial coil, and in the presence of a plane-parallel stratified half-space of conducting materials. The half-space simulates the workpiece, in eddy-current nondestructive evaluation (NDE) parlance. As Figure 1 indicates, the system, composed of the core, coil and half-space, is axisymmetric; this is the simplest, realistic, three-dimensional problem of any degree of generality.

Though the model that we will develop is applicable to arbitrarily shaped bodies-of-revolution, we will specifically attack the problems posed by the core shapes of Figures 2 and 3. The E-shaped core of Figure 2 is typically used in low-frequency eddy-current NDE work, whereas the truncated cylinder of Figure 3 is used in high-frequency work. Again, the problems posed by Figures 2 and 3 possess an axis of rotational symmetry.

If the excitation of the ferrite is weak then the problem may be treated as linear, which means, among other things, that there will be no harmonic distortion of single-frequency sinusoidal signals. At the outset of this investigation we make the small-signal, linearized assumption, but we intend to lay out the appropriate paths to follow in dealing with the more general nonlinear problem.

Cores that are made from powdered ferrite materials are isotropic, but those made from single crystal ferrites are anisotropic. The mathematical approach that we use in developing the model will be sufficiently general that it could include anisotropic core materials, as well.

The problem solved by Dodd, et al. [1-3] differs from ours in that the ferrite core is absent. Thus, in the problem they solved the

excitation source was also parallel to the workpiece (i.e., there was no irregularly shaped core to destroy the plane-parallel symmetry) and this permitted them to solve analytically a number of important problems. We can follow their analytical approach only so far (that point being the determination of a Green's function), and then we must continue with a numerical approach in order to compute the magnetization within the ferrite core. Having computed the core magnetization, we can compute the fields within the workpiece analytically, as well as the driving-point impedance of the coil/core combination.

In a sense, Dodd et al.'s work brought eddy-current NDE "of age" by showing how one could get useful analytical results based on a rigorous application of electromagnetic field theory. In this paper we extend the application of electromagnetic field theory to include numerical techniques for analyzing the fields produced by complex structures. Our approach is very much in the spirit of contemporary research in problem-solving in electromagnetics [4,5].

We start by replacing the ferrite core by an equivalent controlled source of Amperian currents, which, together with the true current in the exciting coil, comprise the total source of the electromagnetic field. The field is expressed as an integral over the regions occupied by the source currents, i.e., the core and coil. The integrand is a vector function of two arguments, one the source point occupied by the currents, and the other argument being the field point at which the electromagnetic field is to be evaluated. The Green's function computed by Dodd, et al., makes its appearance in this integral expression.

The controlled Amperian source current density is not known a priori, however, because it depends on the value of the field at the source point. Hence, we end up with an equation whose unknown appears both outside and inside an integral operator--an integral equation for the unknown Amperian source current density (which is directly related to the magnetization of the ferrite core). This integral equation is reduced to an algebraic system by the method of moments [6], and is then solved using a linear equation solver. Having the Amperian and true currents, we can compute the electromagnetic field at any point of space, including within the

workpiece, by straightforward integration. The derivation of the integral equation and other analytical matters are the subject of Section II.

The transformation of the integral equation by means of the method of moments is dealt with in Section III, and Section IV discusses some of the important numerical matters, such as computation of special functions and infinite integrals, that are crucial to the model.

Results of the model are presented in Section V. In particular, we show the approximate $\overline{B}$ field within the two cores, the driving-point impedance as a function of frequency and the induced eddy-currents as a function of radial coordinate and depth within the workplace.

A section on comments and extensions of the model concludes the paper.

II. ANALYSIS

(a) Derivation of the Volume Integral Equation

In the sinusoidal steady-state, Maxwell's equations are:

$$\nabla \times \overline{E} = -j\omega\overline{B} \qquad (1)(a)$$

$$\nabla \times \overline{H} = j\omega\varepsilon_0\overline{E} + \overline{J} \qquad (b)$$

But $\overline{H} = \overline{B}/\mu_0 - \overline{M}$, so that (1)(b) becomes

$$\nabla \times \overline{B} = j\omega\mu_0\varepsilon_0\overline{E} + \mu_0\nabla\times\overline{M} + \mu_0\overline{J} \qquad (2)$$

In (1) and (2) $\overline{E}$ is the electric field intensity, $\overline{B}$ the magnetic induction, $\overline{H}$ the magnetic field intensity, $\overline{M}$ the magnetization (or magnetic dipole-moment per unit volume) and $\overline{J}$ is the true electric current density. The curl of $\overline{M}$ in (2) clearly plays the same role as $\overline{J}$ in serving as a source for $\overline{B}$; this source term is the Amperian current density. It will play a fundamental role in the integral equation.

Now let $\overline{B} = \nabla \times \overline{A}$, $\overline{E} = -j\omega\overline{A}$, where $\overline{A} = A\overline{a}_\phi$ is the vector potential. It has only a ϕ-component because the current density, $\overline{J}$, does also. Thus,

$\bar{A}$ (and $\bar{E}$) are solenoidal as long as the current density is. When these new definitions are substituted into (2), we obtain the fundamental vector wave equation for $\bar{A}$:

$$\nabla \times \nabla \times \bar{A} = k_0^2 \bar{A} + \mu_0 \nabla \times \bar{M} + \mu_0 \bar{J} \tag{3}$$

The parameter $k_0^2 = \omega^2 \mu_0 \varepsilon_0$ in air; within the workpiece the vector wave equation for $\bar{A}$ is the same as (3), except that $\bar{M} = 0$ and $k_1^2 = \omega^2 \mu_0 \varepsilon_0 - j\omega \mu_0 \sigma$, where σ is the electrical conductivity of the workpiece (we are assuming that the workpiece is a homogeneous half-space). The magnetic permeability of the workpiece is the same as that of free-space, μ_0, which means that the workpiece is nonmagnetic (though this is not an important restriction), and the dielectric constant of the workpiece will simply be assumed to be ε_0. Thoughout this development we include the displacement current density, though it is negligible at the frequencies of interest, even in air.

We begin the analysis by stating the vector Green's identity:

$$\iiint_V [\bar{P} \cdot \nabla \times \nabla \times \bar{Q} - \bar{Q} \cdot \nabla \times \nabla \times \bar{P}] dV =$$

$$\oint_S [\bar{W} \times \nabla \times \bar{P} - \bar{P} \times \nabla \times \bar{Q}] \cdot \bar{a}_n dS \tag{4}$$

where the vector fields, $\bar{P}$ and $\bar{Q}$, are arbitrary, except that they must be well-behaved within V and on S. We are going to apply this identity to certain Green's functions and vector fields, the vector fields being the $\bar{A}$-fields, which satisfy

$$\nabla \times \nabla \times \bar{A}_1 - k_0^2 \bar{A}_1 = \mu_0 \nabla \times \bar{M} + \mu_0 \bar{J}, \quad \nabla \times \nabla \times \bar{A}_2 - k_1^2 \bar{A}_2 = 0, \tag{5}$$

in regions 1 and 2, respectively (see Figure 4). The Green's functions satisfy

$$\nabla \times \nabla \times \bar{G}_{11} - k_0^2 \bar{G}_{11} = \frac{\delta(r-r')\delta(z-z')}{2\pi r'} \bar{a}_\phi, \qquad \begin{matrix} (r',z') \text{ in } 1 \\ (r,z) \text{ in } 1 \end{matrix} \tag{6}(a)$$

$$\nabla \times \nabla \times \bar{G}_{21} - k_1^2 \bar{G}_{21} = 0, \qquad \begin{matrix}(r',z') \text{ in } 1 \\ (r,z) \text{ in } 2\end{matrix} \qquad (b)$$

Clearly, the Green's function is the response to a circular filament of current of radius r' located on the plane $z = z'$. The notation $\bar{G}_{ij}(r,z;\, r',z')$ denotes that the field point (r,z) lies in region i, and the source point (r',z') lies in region j, as shown in Figure 4.

Now apply the vector Green's identity to (5) and (6), letting $\bar{P} = \bar{G}$. and $\bar{G} = \bar{A}$. The volume of integration, V, must be broken into two parts, corresponding to the two regions of Figure 4. The reason for this is that the materials differ from region to region, and so the field vectors will experience certain discontinuities at the surface separating the two regions (z=0, in Figure 4). Hence, over region 1 we have

$$\bar{G}_{11} \cdot \nabla \times \nabla \times \bar{A}_1 = k_0^2 \bar{A}_1 \cdot \bar{G}_{11} + \mu_0 \bar{G}_{11} \cdot \nabla \times \bar{M} + \mu_0 \bar{G}_{11} \cdot \bar{J}$$

$$\bar{A}_1 \cdot \nabla \times \nabla \times \bar{G}_{11} = k_0^2 \bar{A}_1 \cdot \bar{G}_{11} + \frac{\delta(r-r')\delta(z-z')}{2\pi r'} \bar{a}_\phi \cdot \bar{A}_1 \quad .$$

The volume integrand over region 1 becomes, therefore:

$$\mu_0 \bar{G}_{11} \cdot \bar{J} + \mu_0 \bar{G}_{11} \cdot \nabla \times \bar{M} - \frac{\delta(r-r')\delta(z-z')}{2\pi r'} A_1 \quad ,$$

where $\bar{A}_1 = A_1 \bar{a}_\phi$. Now we integrate with respect to the field variables (r,z,ϕ), and get:

$$\iiint_{V_1} [\mu_0 \bar{G}_{11} \cdot \bar{J} + \mu_0 \bar{G}_{11} \cdot \nabla \times \bar{M} - \frac{\delta(r-r')\delta(z-z')}{2\pi r'} A_1] dV =$$

$$\oiint_{S_1} [\bar{A}_1 \times \nabla \times \bar{G}_{11} - \bar{G}_{11} \times \nabla \times \bar{A}_1] \cdot \bar{a}_n dS. \qquad (7)$$

The surface S_1 consists of the z-axis, the infinite spherical sector, S_∞, and the surface $z = 0$, as shown in Figure 4. The integral along the z-axis vanishes because there is zero surface area there, and we assume that there exist no singular sources concentrated along the axis. The

integral along S_∞ vanishes because the fields $\bar{A}_1$ and $\bar{G}_{11}$ satisfy a radiation condition at infinity, which means that there are outgoing waves, only, at infinity. This leaves only the integral along z = 0, which can be written:

$$-2\pi\int_0^\infty [\bar{A}_1 \times \nabla \times \bar{G}_{11} - \bar{G}_{11} \times \nabla \times \bar{A}_1] \Big|_{z=0} \cdot \bar{a}_z \, r\,dr \quad .$$

Hence, we have

$$A_1(r',z') = 2\pi\mu_0 \iint_{coil} \bar{J}(r,z) \cdot \bar{G}_{11}(r,z;\, r',z')\, r\,dr\,dz +$$

$$+ 2\pi\mu_0 \iint_{core} \nabla \times \bar{M}(r,z) \cdot \bar{G}_{11}(r,z;\, r',z')\, r\,dr\,dz + 2\pi \cdot$$

$$\cdot \int_0^\infty [\bar{A}_1(r,z) \times \nabla \times \bar{G}_{11}(r,z;\, r',z') -$$

$$- \bar{G}_{11}(r,z;\, r',z') \times \nabla \times \bar{A}_1(r,z)] \Big|_{z=0} \cdot \bar{a}_z r\,dr \qquad (8)$$

for the result of the integration over V_1, assuming that (r',z') lies in V_1 (recall the meaning of $\bar{G}_{11}$: both field and source points lie in V_1). Note that both the core and coil lie in region 1.

Now we continue with the application of Green's vector identity to region 2. Here we use the second equation in (5), together with (6)(b). Keeping in mind that the source point, (r',z'), still lies within region 1, we get, after arguing as before:

$$0 = 2\pi\int_0^\infty [\bar{A}_2(r,z) \times \nabla \times \bar{G}_{21}(r,z;\, r',z') - \bar{G}_{21}(r,z;\, r',z') \times \nabla \times \bar{A}_2(r,z)] \Big|_{z=0} \cdot$$

$$\cdot \bar{a}_z r\,dr \qquad (9)$$

This integral, however, is proportional to the third integral in (8), as the following argument shows. Use the scalar triple-product to rewrite the integrand in (9) as

$$[(\bar{a}_z \times \bar{A}_2) \cdot \nabla \times \bar{G}_{21} - (\bar{a}_z \times \bar{G}_{21}) \cdot \nabla \times \bar{A}_2]_{z=0} \tag{10}$$

Now $\bar{a}_z \times \bar{A}$ is the tangential component of $\bar{A}$, which is proportional to the tangential component of $\bar{E}$, which must be continuous at the boundry, $z = 0$. Hence,

$$\bar{a}_z \times \bar{A}_2 = \bar{a}_z \times \bar{A}_1$$

at $z = 0$. This is also the first boundary condition to be imposed on $\bar{G}$:

$$\bar{a}_z \times \bar{G}_{21} = \bar{a}_z \times \bar{G}_{11}$$

at $z = 0$. Therefore, (10) becomes

$$[(\bar{a}_z \times \bar{A}_1) \cdot \nabla \times \bar{G}_{21} - (\bar{a}_z \times \bar{G}_{11}) \cdot \nabla \times \bar{A}_2] \Big|_{z=0} =$$

$$[-(\bar{a}_z \times \nabla \times \bar{G}_{21}) \cdot \bar{A}_1 + (\bar{a}_z \times \nabla \times \bar{A}_2) \cdot \bar{G}_{11}] \Big|_{z=0} , \tag{11}$$

where we have again invoked the scalar triple-product. We note that

$$\frac{1}{\mu_1} \bar{a}_z \times \nabla \times \bar{A}_2 \Big|_{z=0} = \frac{1}{\mu_0} \bar{a}_z \times \nabla \times \bar{A}_1 \Big|_{z=0} ,$$

which expresses the continuity of the tangential $\bar{H}$-fields at $z = 0$. Again, we impose the same boundary condition on $\bar{G}$:

$$\frac{1}{\mu_1} \bar{a}_z \times \nabla \times \bar{G}_{21} \Big|_{z=0} = \frac{1}{\mu_0} \bar{a}_z \times \nabla \times \bar{G}_{11} \Big|_{z=0} ,$$

and when this is put into the right-hand side of (11), we get

$$\frac{\mu_1}{\mu_0}\left[-(\bar{a}_z \times \nabla \times \bar{G}_{11}) \cdot \bar{A}_1 + (\bar{a}_z \times \nabla \times \bar{A}_1) \cdot \bar{G}_{11}\right]\Big|_{z=0} =$$

$$\frac{\mu_1}{\mu_0}\left[\bar{A}_1 \times \nabla \times \bar{G}_{11} - \bar{G}_{11} \times \nabla \times \bar{A}_1\right]\Big|_{z=0} \cdot \bar{a}_z \quad ,$$

which is μ_1/μ_0 times the integrand of the third integral in (8), as we set out to prove. Hence, because (9) vanishes, so does the third integral in (8).

To summarize, therefore, upon imposing the boundary conditions at $z = 0$:

$$\bar{a}_z \times \bar{G}_{21}(r,z;\, r',z') = \bar{a}_z \times \bar{G}_{11}(r,z;\, r',z') \qquad (12)$$

$$\frac{1}{\mu_1}\,\bar{a}_z \times \nabla \times \bar{G}_{21}(r,z;\, r',z') = \frac{1}{\mu_0}\,\bar{a}_z \times \nabla \times \bar{G}_{11}(r,z;\, r',z')$$

then (8) becomes

$$A_1(r',\, z') = 2\pi\mu_0 \iint_{\text{coil}} \bar{J}(r,z) \cdot \bar{G}_{11}(r,z;\, r',z')\,r\,dr\,dz$$

$$+ 2\pi\mu_0 \iint_{\text{core}} \nabla \times \bar{M}(r,z) \cdot \bar{G}_{11}(r,z;\, r',z')\,r\,dr\,dz \quad . \qquad (13)$$

We emphasize that the differential operation in (12)(b) is with respect to the field variables, (r,z). From here on we take $\mu_0 = \mu_1$, as we stated earlier.

The magnetic induction is the curl of $\bar{A}$:

$$\bar{B}(r,z) = \nabla \times \bar{A}(r,z)$$

$$= \nabla \times \left\{ \bar{a}_\phi 2\pi\mu_0 \iint_{coil} \bar{G}_{11}(r,z;\, r'z') \cdot \bar{J}(r',z')r'dr'dz' \right\}$$

$$+ \nabla \times \left\{ \bar{a}_\phi 2\pi\mu_0 \iint_{core} \bar{G}_{11}(r,z;\, r',z') \cdot \nabla' \times \bar{M}(r',z')r'dr'dz' \right\} , \quad (14)$$

where we have used the symmetry of $\bar{G}_{11}$:

$$\bar{G}_{11}(r,z;\, r',z') = \bar{G}_{11}(r',z';\, r,z) \quad ,$$

and we note that the curl operation is with respect to the primed variables under the integral sign, and with respect to the field variables (the unprimed variables) outside the integral sign.

The first term of (14) is the incident field, $\bar{B}^{(i)}$, due to the coil, and the second is the scattered field, $\bar{B}^{(s)}$, due to the induced polarization, $\bar{M}$. We proceed to reduce $\bar{B}^{(s)}$. Start with the vector identity

$$\bar{G}_{11}(r,z;\, r',z') \cdot \nabla' \times \bar{M}(r',z') = -\nabla' \cdot \left\{ \bar{G}_{11}(r,z;\, r',z') \times \bar{M}(r',z') \right\}$$

$$+ \bar{M}(r',z') \cdot \nabla' \times \bar{G}_{11}(r,z;\, r',z') \quad , \qquad (15)$$

and write $\bar{B}^{(s)}(r,z)$ as:

$$\bar{B}^{(s)}(r,z) = 2\pi\mu_0 \nabla \times \left\{ \bar{a}_\phi \iint_{core} \bar{M}(r',z') \cdot \nabla' \times \bar{G}_{11}(r,z;\, r',z')r'dr'dz' \right.$$

$$\left. - \bar{a}_\phi \iint_{core} \nabla' \cdot [\bar{G}_{11}(r,z;\, r',z') \times \bar{M}(r',z')]r'dr'dz' \right\}. \quad (16)$$

Upon using Gauss' theorem on the second integral, and extending the surface of the core slightly beyond the (finite) support of $\bar{M}$ ($\bar{M}$ is smooth, so that Gauss' theorem is applicable), the second integral vanishes. We are left with

$$\bar{B}^{(s)}(r,z) = 2\pi\mu_0 \nabla \times \bar{a}_\phi \iint_{\text{core}} \bar{M}(r',z') \cdot \nabla' \times \bar{\bar{G}}_{11}(r,z;\, r',z')r'dr'dz' \quad (17)$$

The total field satisfies:

$$\bar{B}(r,z) = \bar{B}^{(i)}(r,z) + \bar{B}^{(s)}(r,z)$$

$$= \bar{B}^{(i)}(r,z) + 2\pi\mu_0 \nabla \times \bar{a}_\phi \iint_{\text{core}} \bar{M}(r',z') \cdot \nabla \times \bar{\bar{G}}_{11}(r,z;\, r'z')r'dr'dz' \,. \quad (18)$$

To make this into a volume integral equation for $\bar{B}$ or $\bar{M}$, we note that

$$\bar{M} = \bar{B}/\mu_0 - \bar{H} = \bar{B}\left(\frac{1}{\mu_0} - \frac{1}{\mu}\right) \,,$$

where μ is the permeability of the ferrite, so that (18) yields two equivalent integral equations:

$$\bar{B}(r,z) = \bar{B}^{(i)}(r,z) + 2\pi \nabla \times \bar{a}_\phi \iint_{\text{core}} \left(1 - \frac{\mu_0}{\mu}\right) \bar{B}(r',z') \cdot \nabla' \times$$

$$\times \bar{\bar{G}}_{11}(r,z';r',z')r'dr'dz' \quad (19)(a)$$

$$\left(\frac{\mu\mu_0}{\mu-\mu_0}\right)\bar{M}(r,z) = \bar{B}^{(i)}(r,z) + 2\pi\mu_0 \nabla \times \bar{a}_\phi \iint_{\text{core}}$$

$$\bar{M}(r',z') \cdot \nabla' \times \bar{\bar{G}}_{11}(r,z;\, r',z')r'dr'dz'. \quad (b)$$

In either equation the unknown vector field can be expanded in vector pulse-functions, because the curl operation has been transferred to the Green's function.

The curl operation in the unprimed coordinates will be "mollified," or smoothed, by using an appropriate test-function in the method of moments. To see how this is accomplished, consider, again, the vector identity that was used in (15):

$$\bar{P} \cdot \nabla \times \bar{Q} = - \nabla \cdot (\bar{P} \times \bar{Q}) + \bar{Q} \cdot \nabla \times \bar{P} \quad . \tag{20}$$

If $\bar{P}$ satisfies $\nabla \times \bar{P} = 0$, then (20) becomes $\bar{P} \cdot \nabla \times \bar{Q} = -\nabla \cdot (\bar{P} \times \bar{Q})$. When this result is integrated over a patch of space, and Gauss' theorem invoked, we get

$$\iiint_{\text{Patch}} \bar{P} \cdot \nabla \times \bar{Q} \, dV = - \iint_{\partial\text{Patch}} [\bar{P} \times \bar{Q}] \cdot \bar{a}_n dS \quad . \tag{21}$$

This result is void of differential operators. This is what is meant by "mollifying" an equation. We will use this on (19), treating the bracketed term on the right-hand side as the vector $\bar{Q}$.

(b) Derivation of the Green's Function

The Green's function that appears in the integral equations, (19), satisfies (6) and (12). Because there is only a ϕ-component of $\bar{G}$, these equations, in cylindrical coordinates, reduce to:

$$\frac{\partial^2 G_{11}}{\partial z^2} + \frac{\partial^2 G_{11}}{\partial r^2} + \frac{1}{r}\frac{\partial G_{11}}{\partial r} - \frac{G_{11}}{r} + k_0^2 G_{11} = -\frac{\delta(r-r')\delta(z-z')}{2\pi r'}, \quad 0 < z,z' \tag{22}(a)$$

$$\frac{\partial^2 G_{21}}{\partial z^2} + \frac{\partial^2 G_{21}}{\partial r^2} + \frac{1}{r}\frac{\partial G_{21}}{\partial r} - \frac{G_{21}}{r} + k_1^2 G_{21} = 0 \quad , \qquad z < 0 \tag{b}$$

$$G_{11}(r,0;\, r',z') = G_{21}(r,0;\, r',z') \tag{c}$$

$$\frac{\partial G_{11}}{\partial z}(r,0;\, r',z') = \frac{\partial G_{21}}{\partial z}(r,0;\, r',z') \quad . \tag{d}$$

In going from (12)(b) to (22)(d) we have put $\mu_0 = \mu_1$.

In solving (22)(a) we must consider two subregions of region 1: $z > z'$, $z < z'$. At $z = z'$ we require that the Green's function be continuous, but that there be a discontinuity in its slope. The amount

of discontinuity can be determined by integrating (22)(a) over a small interval about z':

$$\int_{z'-\epsilon}^{z'+\epsilon} [\text{Left-hand side of (22)(a)}]dz \simeq \frac{\partial G_{11}}{\partial z}\Big|_{z'+\epsilon} - \frac{\partial G_{11}}{\partial z}\Big|_{z'-\epsilon} = -\frac{\delta(r-r')}{2\pi r'} .$$

Thus, the discontinuity in slope is given by

$$\frac{\partial G_{11}}{\partial z}\Big|_{z'_+} - \frac{\partial G_{11}}{\partial z}\Big|_{z'_-} = \frac{-\delta(r-r')}{2\pi r'} \quad . \tag{23}$$

The solution of (22) is facilitated by using Bessel transforms. We start by stating the fact that any function, f(r), can be expanded as the double integral

$$f(r) = \int_0^\infty J_n(r\ell)\ell d\ell \int_0^\infty f(\rho)J_n(\ell\rho)\rho d\rho \tag{24}$$

which means that

$$\frac{\delta(r-\rho)}{\rho} = \int_0^\infty J_n(r\ell)J_n(\rho\ell)\ell d\ell \ . \tag{25}$$

The second integral in (24) defines the Bessel transform, $F(\ell)$, of f(r).

We apply the Bessel transform to (22)(a) by writing

$$G_{11}(r,z;\ r',z') = \int_0^\infty \tilde{G}_{11}(\ell,z;\ r',z')J_n(\ell r)\ell d\ell$$

Then

$$\frac{\partial^2 G_{11}}{\partial r^2} + \frac{1}{r}\frac{\partial G_{11}}{\partial r} - \frac{G_{11}}{r^2} = \int_0^\infty \tilde{G}_{11}(\ell,z;\ r',z')\ell^2[J_n''(\ell r)+J_n'(\ell r)/\ell r - J_n(\ell r)/(\ell r)^2]\ell d\ell$$

But $J_1(z)$ satisfies Bessel's equation

$$J_1''(z) + J_1'(z)/z - J_1(z)/z^2 = -J_1(z) \quad .$$

Hence, in the last integral, and hereafter, we let n = 1 and get

$$\frac{\partial^2 G_{11}}{\partial r^2} + \frac{1}{r}\frac{\partial G_{11}}{\partial r} - \frac{G_{11}}{r^2} = -\int_0^\infty \ell^2 \tilde{G}_{11}(\ell,z;\, r',z') J_1(\ell r)\ell d\ell \quad .$$

The z-derivatives are simply

$$\frac{\partial^2 G_{11}}{\partial z^2} = \int_0^\infty \frac{d^2\tilde{G}_{11}}{dz^2}(\ell,z;\, r',z') J_1(\ell r)\ell d\ell \quad .$$

Upon assembling these results, together with (25), into (22)(a), we get

$$\int_0^\infty [\frac{d^2\tilde{G}_{11}}{dz^2} + (k^2-\ell^2)\tilde{G}_{11}] J_1(\ell r)\ell d\ell = -\frac{\delta(z-z')}{2\pi}\int_0^\infty J_1(r\ell)J_1(r'\ell)\ell d\ell \quad . \quad (27)$$

Since this holds for all r we may simply equate integrands to get an ordinary differential equation for the Bessel-transformed Green's function:

$$\frac{d^2\tilde{G}_{11}}{dz^2} + (k_0^2-\ell^2)\tilde{G}_{11} = -\delta(z-z')\frac{J_1(r\ell)}{2\pi} \quad , \qquad 0 < z,z' \quad . \qquad (28)(a)$$

Similarly

$$\frac{d^2\tilde{G}_{21}}{dz^2} + (k_1^2-\ell^2)\tilde{G}_{21} = 0 \quad , \qquad z < 0,\ z' > 0 \quad . \qquad (b)$$

The boundary conditions (22)(c),(d) and the discontinuity condition, (23), when expressed in terms of the Bessel transforms are

$$\tilde{G}_{11}(\ell,0;\ r',z') = \tilde{G}_{21}(\ell,0;\ r',z') \qquad (c)$$

$$\frac{d\tilde{G}_{11}}{dz}(\ell,0;\ r',z') = \frac{d\tilde{G}_{21}}{dz}(\ell,0;\ r',z') \qquad (d)$$

$$\frac{d\tilde{G}_{11}}{dz}(\ell,z'_{+};\ r',z') - \frac{d\tilde{G}_{11}}{dz}(\ell,z'_{-};\ r',z') = \frac{-J_1}{2\pi}(r\ell) \quad . \qquad (e)$$

Also, we have continuity of $\tilde{G}_{11}$ at $z = z'$:

$$\tilde{G}_{11}(\ell,z'_{+};\ r',z') = \tilde{G}_{11}(\ell,z';\ r',z') \qquad (f)$$

Solutions of (28)(a) in the appropriate subregions are:

$$\tilde{G}_{11}(\ell,z;\ r',z') = Ae^{-\alpha_0(z-z')} \qquad , \ z > z' > 0$$

$$= Be^{-\alpha_0(z-z')} + Ce^{\alpha_0(z-z')} \qquad , \ z' > z > 0 \qquad (29)$$

where $\alpha_0 = (\ell^2 - k_0^2)^{1/2}$. Equations (28)(e),(f) are applied to determine relations between the arbitrary constants A, B, C:

$$A - B - C = 0 \qquad (30)(a)$$

$$A - B + C = \frac{J_1(r'\ell)}{2\pi\alpha_0} \quad . \qquad (b)$$

The solution of (28)(b) requires only a single arbitrary constant:

$$\tilde{G}_{21}(\ell,z;\ r',z') = De^{\alpha_1(z-z')} \qquad , \qquad z < 0, \ 0 < z' \quad . \qquad (31)$$

where $\alpha_1 = (\ell^2 - k_1^2)^{1/2}$. When (28)(c),(d) are applied to (29) and (31), we get the final two equations

$$De^{-\alpha_1 z'} = Be^{\alpha_0 z'} + Ce^{-\alpha_0 z'} \qquad (32)(a)$$

$$-\alpha_0 Be^{\alpha_0 z'} + \alpha_0 Ce^{-\alpha_0 z'} = \alpha_1 De^{-\alpha_1 z'} \qquad (b)$$

The solution of (30) and (32) is readily found to be

$$A = \left[\frac{\alpha_0 - \alpha_1}{\alpha_0 + \alpha_1} e^{-2\alpha_0 z'} + 1\right] \frac{J_1(r'\ell)}{4\pi\alpha_0} \qquad (33)(a)$$

$$B = \frac{\alpha_0 - \alpha_1}{\alpha_0 + \alpha_1} \cdot \frac{J_1(r'\ell)e^{-2\alpha_0 z'}}{4\pi\alpha_0} \quad . \qquad (b)$$

$$C = \frac{J_1(r'\ell)}{4\pi\alpha_0} \qquad (c)$$

$$D = \frac{J_1(r'\ell)e^{-(\alpha_0-\alpha_1)z'}}{(\alpha_0+\alpha_1)2\pi} \quad . \qquad (d)$$

The final expression for the Green's functions is obtained by substituting (33) into (29) and (31), and then that result into (26):

$$G_{11}(r,z;\, r',z') = \frac{1}{2\pi}\int_0^\infty \left[\frac{Re^{-\alpha_0(z+z')} + e^{-\alpha_0(z-z')}}{2\alpha_0}\right] J_1(r'\ell)J_1(r\ell)\ell d\ell, \quad z>z'>0$$

$$= \frac{1}{2\pi}\int_0^\infty \left[\frac{Re^{-\alpha_0(z+z')} + e^{\alpha_0(z-z')}}{2\alpha_0}\right] J_1(r'\ell)J_1(r\ell)\ell d\ell, \quad z'>z>0$$

$$= \frac{1}{2\pi} \int_0^\infty \left[\frac{\mathrm{Re}\, e^{-\alpha_0(z+z')} + e^{-\alpha_0|z-z'|}}{2\alpha_0} \right] J_1(r'\ell) J_1(r\ell) \ell d\ell, \quad z,z'>0 \qquad (34)(a)$$

$$G_{21}(r,z;\, r',z') = \frac{1}{2\pi} \int_0^\infty \frac{T}{\alpha_0} e^{(\alpha_1 z - \alpha_0 z')} J_1(r'\ell) J_1(r\ell) \ell d\ell \quad . \qquad (b)$$

We have defined

$$R = \frac{\alpha_0 - \alpha_1}{\alpha_0 + \alpha_1}, \quad T = \frac{\alpha_0}{\alpha_0 + \alpha_1} \qquad (35)$$

in (34). We have already alluded to the fact that G_{11} is symmetrical under interchange of source and field coordinates, and (34)(a) verifies that fact. The final form of G_{11} in (34)(a) is merely a compact representation that includes the first two.

Now that we have the Green's function that is to be used in (19), we can proceed to transform the integral equation into vector-matrix form.

III. REDUCTION OF THE INTEGRAL EQUATION TO VECTOR-MATRIX FORM: THE METHOD OF MOMENTS

From here on we will work with the integral equation (19)(a). The starting point in the numerical reduction of this equation is to partition the core in a regular grid, as shown in Figure 5 for the cylinder. Based on this partition, we expand the unknown field in pulse functions

$$\bar{B}(r,z) = \sum_{j=1}^{N_c} \bar{B}_j P_j(r,z), \qquad (36)$$

or in component form

$$B_r(r,z) = \sum_{j=1}^{N_c} b_j^{(r)} \left(\frac{r}{r_b}\right) P_j(r,z) \qquad (37)(a)$$

$$B_z(r,z) = \sum_{j=1}^{N_c} b_j^{(z)} P_j(r,z) \quad , \qquad (b)$$

where $\{b_j^{(r)}\}$, $\{b_j^{(z)}\}$ are the expansion coefficients for the r- and z-components, N_c is the number of cells in the grid and $P_j(r,z)$ is the jth pulse function, which is defined by

$$P_j(r,z) = 1, \qquad (r,z) \text{ in jth cell} \qquad (39)$$

$$= 0, \qquad \text{otherwise.}$$

Upon substituting (36) into (19)(a), we get

$$\sum_{j=1}^{N_c} \bar{B}_j P_j(r,z) = \bar{B}^{(i)}(r,z) + \sum_{j=1}^{N_c} \nabla \times \bar{a}_\phi 2\pi \iint_{\text{jth cell}}$$

$$\left(1 - \frac{\mu_0}{\mu}\right) \bar{B}_j(r',z') \cdot \nabla' \times \bar{G}_{11}(r,z;\, r',z') r'dr'dz'. \qquad (39)$$

The next step in the method of moments is to take moments of (39), i.e., to multiply (39) by testing-functions and then integrate. For our testing-functions we take the same functions, $\bar{V}P_i(r,z)$, where $\bar{V}$ is either $(r/r_b)\bar{a}_r$ or $\bar{a}_z$, as for expansion, (36). When the same functions are used for expansion and testing, the method is called the Galerkin variant of the method of moments. Thus, the result of taking moments of (39) is

$$\sum_{j=1}^{N_c} \iint_{\text{ith cell}} \bar{V} \cdot \bar{B}_j P_j(r,z) r dr dz = \iint_{\text{ith cell}} \bar{V} \cdot \bar{B}^{(i)}(r,z)\, r dr dz +$$

$$\sum_{j=1}^{N_c} \iint_{\text{ith cell}} \bar{V} \cdot \nabla \times \{\bar{a}_\phi f_j(r,z)\} r dr dz, \qquad (40)$$

where we have written

$$f_j(r,z) = 2\pi \iint_{\text{jth cell}} (1-\frac{\mu_0}{\mu})\bar{B}_j(r',z') \cdot \nabla' \times \bar{G}_{11}(r,z;\, r',z')r'dr'dz'$$

$$= b_j^{(r)} 2\pi \iint_{\text{jth cell}} (1-\frac{\mu_0}{\mu})(\frac{r'}{r_b}) \cdot (\frac{-\partial G_{11}(r,z;\, r',z')}{\partial z'})r'dr'dz'$$

$$+ b_j^{(z)} 2\pi \iint_{\text{jth cell}} (1-\frac{\mu_0}{\mu})\left[\frac{\partial G_{11}(r,z;\, r',z')}{\partial r'} + \frac{G_{11}(r,z;\, r',z')}{r'}\right] r'dr'dz'. \quad (41)$$

Recalling the definition of P_j allows us to reduce the left-hand side of (40) to

$$\delta_{ij} \iint_{\text{ith cell}} \bar{\nabla} \cdot \bar{B}_j r dr dz \quad . \quad (42)$$

The first integral on the right-hand side of (40) becomes the forcing-function vector, $\bar{F}_j$.

Because $\nabla \times \bar{\nabla} = 0$, the second integral on the right-hand side of (40) may be reduced by the use of (21), with the result that the integral becomes

$$\oint_{\text{ith cell}} [\bar{a}_\phi \times \bar{\nabla}] \cdot \bar{a}_n f_j(r,z)dA \quad ,$$

where the contour integral implies an integral over the boundary of a two-dimensional cell. Upon referring to Figure 6, this integral may be written

$$\oint_{\text{ith cell}} [\bar{a}_\phi \times \bar{V}] \cdot \bar{a}_n f_j(r,z)dA = \int_{r_i^{(-)}}^{r_i^{(+)}} f_j(r,z_i^{(+)})(\bar{a}_\phi \times \bar{V}) \cdot \bar{a}_z r dr$$

$$+ \int_{z_i^{(-)}}^{z_i^{(+)}} f_j(r_i^{(+)},z) r_i^{(+)} (\bar{a}_\phi \times \bar{V}) \cdot \bar{a}_r dz - \int_{r_i^{(-)}}^{r_i^{(+)}} f_j(r,z_i^{(-)})(\bar{a}_\phi \times \bar{V}) \cdot \bar{a}_z r dr$$

$$- \int_{z_i^{(-)}}^{z_i^{(+)}} f_j(r_i^{(-)},z) r_i^{(-)} (\bar{a}_\phi \times \bar{V}) \cdot \bar{a}_r dz. \qquad (43)$$

Now we let $\bar{V} = (r/r_b)\bar{a}_r$ in (43), and get

$$\oint_{\text{ith cell}} [\bar{a}_\phi \times \bar{a}_r] \cdot \bar{a}_n (r/r_b) f_j(r,z)dA = \int_{r_i^{(-)}}^{r_i^{(+)}} (r/r_b) f_j(r,z_i^{(-)}) r dr$$

$$- \int_{r_i^{(-)}}^{r_i^{(+)}} (r/r_b) f_j(r,z_i^{(+)}) r dr \; . \qquad (44)(a)$$

Similarly, when $\bar{V} = \bar{a}_z$:

$$\oint_{\text{ith cell}} [\bar{a}_\phi \times \bar{a}_z] \cdot \bar{a}_n f_j(r,z)dA = \int_{z_i^{(-)}}^{z_i^{(+)}} f_j(r_i^{(+)},z) r_i^{(+)} dz -$$

$$\int_{z_i^{(-)}}^{z_i^{(+)}} f_j(r_i^{(-)},z) r_i^{(-)} dz \; . \qquad (44)(b)$$

Upon substituting (41) into (44)(a),(b), we get, respectively,

$$b_j^{(r)} 2\pi \int_{r_i^{(-)}}^{r_i^{(+)}} \left(\frac{r}{r_b}\right) r\,dr \iint_{\text{jth cell}} \left(1 - \frac{\mu_0}{\mu}\right)\left(\frac{r'}{r_b}\right) \cdot$$

$$\cdot \left[\frac{\partial G_{11}(r, z_i^{(+)};\, r', z')}{\partial z'} - \frac{\partial G_{11}(r, z_i^{(-)};\, r', z')}{\partial z'} \right] r'\,dr'\,dz'$$

$$+ b_j^{(z)} 2\pi \int_{r_i^{(-)}}^{r_i^{(+)}} \left(\frac{r}{r_b}\right) r\,dr \iint_{\text{jth cell}} \left(1 - \frac{\mu_0}{\mu}\right) \cdot$$

$$\cdot \left[\frac{\partial G_{11}(r, z_i^{(-)}; r', z')}{\partial r'} + \frac{G_{11}(r, z_i^{(-)};\, r', z')}{r'} \right.$$

$$\left. - \frac{\partial G_{11}(r, z_i^{(+)};\, r', z')}{\partial r'} - \frac{G_{11}(r, z_i^{(+)};\, r', z')}{r'} \right] r'\,dr'\,dz' \qquad (45)(a)$$

$$b_j^{(r)} 2\pi \int_{z_i^{(-)}}^{z_i^{(+)}} dz \iint_{\text{jth cell}} \left(1 - \frac{\mu_0}{\mu}\right)\left(\frac{r'}{r_b}\right) \cdot$$

$$\cdot \left[r_i^{(-)} \frac{\partial G_{11}(r_i^{(-)}, z;\, r', z')}{\partial z'} - r_i^{(+)} \frac{\partial G_{11}(r_i^{(+)}, z;\, r', z')}{\partial z'} \right] r'\,dr'\,dz'$$

$$+ b_j^{(z)} 2\pi \int_{z_i^{(-)}}^{z_i^{(+)}} dz \iint_{\text{jth cell}} \left(1 - \frac{\mu_0}{\mu}\right) \cdot$$

$$\cdot \left\{ r_i^{(+)} \left[\frac{\partial G_{11}(r_i^{(+)}, z;\, r', z')}{\partial r'} + \frac{G_{11}(r_i^{(+)}, z;\, r', z')}{r'} \right] \right.$$

$$\left. - r_i^{(-)} \left[\frac{\partial G_{11}(r_i^{(-)}, z;\, r', z')}{\partial r'} + \frac{G_{11}(r_i^{(-)}, z;\, r', z')}{r'} \right] \right\} r'\,dr'\,dz' \qquad (b)$$

We can now start to assemble the matrix equations. When $\bar{V} = (r/r_b)\bar{a}_r$ in (40) we get, upon using (42) and (45):

$$b_i^{(r)} \iint_{\text{ith cell}} (\frac{r}{r_b})^2 r dr dz = 2\pi\mu_0 \int_{r_i^{(-)}}^{r_i^{(+)}} (\frac{r}{r_b}) r dr \iint_{\text{coil}} \cdot$$

$$\cdot [G_{11}(r,z_i^{(-)}; r',z') - G_{11}(r,z_i^{(+)}; r',z')] J(r',z') r' dr' dz'$$

$$+ \sum_{j=1}^{N_c} b_j^{(r)} 2\pi \int_{r_i^{(-)}}^{r_i^{(+)}} (\frac{r}{r_b}) r dr \iint_{\text{jth cell}} (1 - \frac{\mu_0}{\mu})(\frac{r'}{r_b}) \cdot$$

$$\cdot \left[\frac{\partial G_{11}(r,z_i^{(+)}; r',z')}{\partial z'} - \frac{\partial G_{11}(r,z_i^{(-)}; r',z')}{\partial z'} \right] r' dr' dz'$$

$$+ \sum_{j=1}^{N_c} b_j^{(z)} 2\pi \int_{r_i^{(-)}}^{r_i^{(+)}} (\frac{r}{r_b}) r dr \iint_{\text{jth cell}} (1 - \frac{\mu_0}{\mu}) \cdot$$

$$\cdot \left[\frac{\partial G_{11}(r,z_i^{(-)}; r',z')}{r'} + \frac{G_{11}(r,z_i^{(-)}; r',z')}{r'} \right.$$

$$\left. - \frac{\partial G_{11}(r,z_i^{(+)}; r',z')}{\partial r'} - \frac{G_{11}(r,z_i^{(+)}; r',z')}{r'} \right] r' dr' dz'$$

$$i = 1, \ldots, N_c \qquad (46)(a)$$

and when $\bar{V} = \bar{a}_z$, (40) becomes

$$b_i^{(z)} \iint_{\text{ith cell}} r\,dr\,dz = 2\pi\mu_0 \int_{z_i^{(-)}}^{z_i^{(+)}} dz \iint_{\text{coil}} \cdot$$

$$\cdot \left[r_i^{(+)} G_{11}(r_i^{(+)}, z;\, r', z') - r_i^{(-)} G_{11}(r_i^{(-)}, z;\, r', z')\right] J(r', z')\, r'\,dr'\,dz'$$

$$+ \sum_{j=1}^{N_c} b_j^{(r)} 2\pi \int_{z_i^{(-)}}^{z_i^{(+)}} dz \iint_{\text{jth cell}} \left(1 - \frac{\mu_0}{\mu}\right)\left(\frac{r'}{r_b}\right) \cdot$$

$$\cdot \left[r_i^{(-)} \frac{\partial G_{11}(r_i^{(-)}, z;\, r', z')}{\partial z'} - r_i^{(+)} \frac{\partial G_{11}(r_i^{(+)}, z;\, r', z')}{\partial z'}\right] r'\,dr'\,dz'$$

$$+ \sum_{j=1}^{N_c} b_j^{(z)} 2\pi \int_{z_i^{(-)}}^{z_i^{(+)}} dz \iint_{\text{jth cell}} \left(1 - \frac{\mu_0}{\mu}\right) \cdot$$

$$\cdot \left\{r_i^{(+)} \left[\frac{\partial G_{11}(r_i^{(+)}, z;\, r', z')}{\partial r'} + \frac{G_{11}(r_i^{(+)}, z;\, r', z')}{r'}\right]\right.$$

$$\left. - r_i^{(-)} \left[\frac{\partial G_{11}(r_i^{(-)}, z;\, r', z')}{\partial r'} + \frac{G_{11}(r_i^{(-)}, z;\, r', z')}{r'}\right]\right\} r'\,dr'\,dz'$$

$$i = 1, \ldots, N_c, \quad (46)(b)$$

where the first term on the right-hand side of these equations comes from substituting $\bar{B}^{(i)}$ in (14), into the first term on the right-hand side of (40), and then using (21) to mollify the term, as before.

These equations can be put into the following matrix form:

$$\left[\begin{array}{c|c} A^{(rr)} - G^{(rr)} & -G^{(rz)} \\ \hline -G^{(zr)} & A^{(zz)} - G^{(zz)} \end{array}\right] \left[\begin{array}{c} b^{(r)} \\ \hline b^{(z)} \end{array}\right] = \left[\begin{array}{c} F^{(r)} \\ \hline F^{(z)} \end{array}\right] \quad . \quad (47)$$

The overall system-matrix is of order $2N_c \times 2N_c$.

The elements of the submatrices and forcing-function vectors can be reduced to infinite integrals by substituting the Green's function, (34)(a), and its curl-components, into (46). The components of $\nabla_x \bar{G}_{11}$ are given by

$$\frac{\partial G_{11}(r,z;\, r',z')}{\partial z'} = \frac{1}{2\pi} \int_0^\infty \left[\frac{-Re^{-\alpha_0(z+z')} \mp e^{-\alpha_0|z-z'|}}{2}\right] J_1(r'\ell) J_1(r\ell)\ell d\ell$$

$$(-):\ z' > z$$

$$(+):\ z > z' \qquad (48)(a)$$

$$\frac{\partial G_{11}(r,z;\, r',z')}{\partial r'} + \frac{G_{11}(r,z;\, r',z')}{r'} = \frac{1}{2\pi} \int_0^\infty \left[\frac{Re^{-\alpha_0(z+z')} + e^{-\alpha_0|z-z'|}}{2\alpha_0}\right] J_0(r'\ell) \cdot$$

$$\cdot\, J_1(r\ell)\ell d\ell \quad . \qquad (b)$$

In evaluating the integrals that define the matrix elements, we interchange the orders of integration with respect to (r,z, r',z') in (46) and those with respect to the transform variable, ℓ. The results are:

$$F_i^{(r)} = \frac{\mu_0 n_c I}{r_b} \int_0^\infty \left[\frac{R}{2} F_1(z_1,z_2) F_1(z_i^{(-)}, z_i^{(+)}) + \frac{F_2(z_1,z_2,z_i^{(-)}) - F_2(z_1,z_2,z_i^{(+)})}{2\alpha_0}\right] \cdot$$

$$\cdot \frac{I(r_1\ell, r_2\ell) B_2(r_i^{(-)}\ell, r_i^{(+)}\ell)}{\ell^4}\, d\ell \qquad (49)(a)$$

$$F_i^{(z)} = \mu_0 n_c I \int_0^\infty \left[\frac{RF_1(z_1,z_2)F_1(z_i^{(-)},z_i^{(+)}) + F_3(z_1,z_2,z_i^{(-)},z_i^{(+)})}{2\alpha_0}\right] B_1(r_i^{(-)}\ell, r_i^{(+)}\ell) \cdot$$

$$\cdot \frac{I(r_1\ell, r_2\ell)}{\ell^2}\, d\ell \qquad \text{(b)}$$

$$G_{ij}^{(rr)} = (1-\frac{\mu_0}{\mu}) \cdot \frac{1}{r_b^2} \int_0^\infty \cdot$$

$$\cdot \left[\frac{R\alpha_0 F_1(z_j^{(-)},z_j^{(+)})F_1(z_i^{(-)},z_i^{(+)}) + F_4(z_j^{(-)},z_j^{(+)},z_i^{(-)}) - F_4(z_j^{(-)},z_j^{(+)},z_i^{(+)})}{2}\right]$$

$$\cdot \frac{B_2(\ell r_j^{(-)},\ell r_j^{(+)})B_2(\ell r_i^{(-)},\ell r_i^{(+)})}{\ell^5}\, d\ell \qquad \text{(c)}$$

$$G_{ij}^{(zz)} = (1-\frac{\mu_0}{\mu}) \int_0^\infty \left[\frac{RF_1(z_i^{(-)},z_i^{(+)})F_1(z_j^{(-)},z_j^{(+)}) + F_3(z_i^{(-)},z_i^{(+)},z_j^{(-)},z_j^{(+)})}{2\alpha_0}\right] \cdot$$

$$\cdot \frac{B_1(\ell r_j^{(-)},\ell r_j^{(+)})B_1(\ell r_i^{(-)},\ell r_i^{(+)})}{\ell}\, d\ell \qquad \text{(d)}$$

$$G_{ij}^{(rz)} = (1-\frac{\mu_0}{\mu}) \cdot \frac{1}{r_b} \int_0^\infty \cdot$$

$$\cdot \left[\frac{R}{2} F_1(z_j^{(-)},z_j^{(+)})F_1(z_i^{(-)},z_i^{(+)}) + \frac{F_2(z_i^{(-)},z_i^{(+)},z_i^{(-)}) - F_2(z_i^{(-)},z_i^{(+)},z_i^{(+)})}{2\alpha_0}\right]$$

$$\cdot \frac{B_2(\ell r_i^{(-)},\ell r_i^{(+)})B_1(\ell r_i^{(-)},\ell r_i^{(+)})}{\ell^3}\, d\ell \qquad \text{(e)}$$

$$G_{ij}^{(zr)} = (1 - \frac{\mu_0}{\mu}) \cdot \frac{1}{r_b} \int_0^\infty \left[\frac{RF_1(z_i^{(-)}, z_i^{(+)}) F_1(z_j^{(-)}, z_j^{(+)}) + F_5(z_i^{(-)}, z_i^{(+)}, z_j^{(-)}, z_j^{(+)})}{2} \right] \cdot$$

$$\cdot \frac{B_2(\ell r_j^{(-)}, \ell r_j^{(+)}) B_1(\ell r_i^{(-)}, \ell r_i^{(+)})}{\ell^3} \, d\ell \qquad (f)$$

$$A_{ij}^{(rr)} = \delta_{ij} \int_{z_i^{(-)}}^{z_i^{(+)}} dz \int_{r_i^{(-)}}^{r_i^{(+)}} (\frac{r}{r_b})^2 r dr = \delta_{ij} r_b^2 (z_i^{(+)} - z_i^{(-)}) \cdot \frac{(r_i^{(+)}/r_b)^4 - (r_i^{(-)}/r_b)^4}{4} \qquad (g)$$

$$A_{ij}^{(zz)} = \delta_{ij} \int_{z_i^{(-)}}^{z_i^{(+)}} dz \int_{r_i^{(-)}}^{r_i^{(+)}} r dr = \delta_{ij} r_b^2 (z_i^{(+)} - z_i^{(-)}) \cdot \frac{(r_i^{(+)}/r_b)^2 - (r_i^{(-)}/r_b)^2}{2} \qquad (h)$$

The functions used in (49) are defined here:

$$F_1(a,b) = \int_a^b e^{-\alpha_0 z} \, dz = \frac{e^{-\alpha_0 a} - e^{-\alpha_0 b}}{\alpha_0} \qquad (50)(a)$$

$$F_2(a,b,c) = \int_a^b e^{-\alpha_0 |c-z|} \, dz = \frac{e^{-\alpha_0 (a-c)} - e^{-\alpha_0 (b-c)}}{\alpha_0}, \qquad c \leq a$$

$$= \frac{2 - e^{-\alpha_0 (c-a)} - e^{-\alpha_0 (b-c)}}{\alpha_0}, \qquad a \leq c \leq b$$

$$= \frac{e^{-\alpha_0 (c-b)} - e^{-\alpha_0 (c-a)}}{\alpha_0}, \qquad b \leq c \qquad (b)$$

$$F_3(z_1,z_2,z_i^{(-)},z_i^{(+)}) = \int_{z_1}^{z_2} dz' \int_{z_i^{(-)}}^{z_i^{(+)}} dz e^{-\alpha_0|z-z'|} = I_1 + I_2 + I_3 + I_4 \ ,$$

$$I_1 = -2x_1/\alpha_0 - e^{-\alpha_0 x_1}/\alpha_0^2 \quad , \quad x_1 > 0 \ , \quad x_1 = z_i^{(+)} - z_2$$

$$= -e^{\alpha_0 x_1}/\alpha_0^2 \quad , \quad x_1 < 0$$

$$I_2 = -2x_2/\alpha_0 - e^{-\alpha_0 x_2}/\alpha_0^2 \quad , \quad x_2 > 0 \ , \quad x_2 = z_i^{(-)} - z_1$$

$$= -e^{\alpha_0 x_2}/\alpha_0^2 \quad , \quad x_2 < 0$$

$$I_3 = 2x_3/\alpha_0 + e^{-\alpha_0 x_3}/\alpha_0^2 \quad , \quad x_3 > 0 \ , \quad x_3 = z_i^{(-)} - z_2$$

$$= e^{\alpha_0 x_3}/\alpha_0^2 \quad , \quad x_3 < 0$$

$$I_4 = 2x_4/\alpha_0 + e^{-\alpha_0 x_4}/\alpha_0^2 \quad , \quad x_4 > 0 \ , \quad x_4 = z_i^{(+)} - z_1$$

$$= e^{\alpha_0 x_4}/\alpha_0^2 \quad , \quad x_4 < 0 \qquad (c)$$

$$F_4(a,b,c) = \int_a^b (\pm e^{-\alpha_0|c-z|}) \, dz, \qquad (+): \ c < z \qquad (-): \ z < c$$

$$= \frac{e^{-\alpha_0(a-c)} - e^{-\alpha_0(b-c)}}{\alpha_0} \ , \qquad c \leq a \qquad (d)$$

$$= \frac{e^{-\alpha_0(c-a)} - e^{-\alpha_0(b-c)}}{\alpha_0} , \qquad a \leq c \leq b$$

$$= \frac{e^{-\alpha_0(c-a)} - e^{-\alpha_0(c-b)}}{\alpha_0} , \qquad b \leq c \tag{d}$$

$$F_5(a,b,c,d) = \int_a^b dz \int_c^d dz' \left(\pm e^{-\alpha_0|z-z'|}\right) , \qquad \begin{matrix}(+): z < z' \\ (-): z' < z\end{matrix}$$

$$= \frac{F_2(a,b,c) - F_2(a,b,d)}{\alpha_0} \tag{e}$$

$$B_1(a,b) = \int_a^b zJ_0(z)dz = bJ_1(b) - aJ_1(a) \tag{f}$$

$$B_2(a,b) = \int_a^b z^2J_1(z)dz = b^2J_2(b) - a^2J_2(a) \tag{g}$$

$$I(a,b) = \int_a^b zJ_1(z)dz \tag{h}$$

We will discuss the computation of the last three functions in the next section.

An interesting feature of the matrices in (49) is their symmetry relations:

$$G_{ij}^{(rr)} = G_{ji}^{(rr)}, \; G_{ij}^{(zz)} = G_{ji}^{(zz)}, \; G_{ij}^{(rz)} = G_{ji}^{(zr)} . \tag{51}$$

These relations, which reduce the time to compute and fill the system-matrix, are a result of using the Galerkin variant of the method of moments.

In deriving the forcing-function vector in (49)(a),(b), we assumed that the coil is uniformly and densely wound with n_c turns per unit area, that it occupies the rectangle $r_1 < r < r_2$, $z_1 < z < z_2$, and that it carries a current of I amperes.

IV. NUMERICAL ANALYSIS: COMPUTATION OF SPECIAL FUNCTIONS AND INTEGRALS

The method of moments, or any other scheme that is used to generate numbers, depends critically on effective numerical methods. The end result of the method of moments is the vector-matrix equation (47). We solve this equation very efficiently by using a linear equation solver that employs the Crout algorithm to factor the system-matrix (we do not use matrix inversion, because that is less efficient). The algorithm uses scaled partial pivoting and back substitution; it is implemented in complex double-precision on the computer.

(a) Computation of Special Functions

The Bessel functions, $J_0(z)$, $J_1(z)$, $J_2(z)$, that appear throughout the vector-matrix elements of (49), are easily computed by appealing to a series expansion when abs(z) < 10, and to well known asymptotic expansions when abs(z) > 10 [7, Ch. 9].

The computation of the Bessel-function integral, (50)(h), is based on the fact that [8, Vol. 1, p. 219]:

$$\int_0^z t^m J_n(t)\,dt = \frac{z^{m+n+1}}{2^n (m+n+1)\,\Gamma(n+1)} \; {}_1F_2\left(\begin{matrix} (m+n+1)/2 \\ (m+n+3)/2,\ n+1 \end{matrix} \middle| \; \frac{-z^2}{4} \right), \qquad (52)$$

where z is a complex number and ${}_1F_2$ is a generalized hypergeometric function. Here, m = n = 1, so that

$$\int_0^z t J_1(t)\,dt = \frac{z^3}{6} \; {}_1F_2\left(\begin{matrix} 3/2 \\ 5/2,\ 2 \end{matrix} \middle| \; \frac{-z^2}{4} \right). \qquad (53)$$

Now

$$ {}_1F_2\left(\begin{matrix} 3/2 \\ 5/2, \quad 2 \end{matrix} \middle| \frac{-z^2}{4} \right) = \sum_{k=0}^{\infty} a_k \quad , \tag{54} $$

where

$$ a_0 = 1, \quad a_k = \frac{(-z^2/4)^k}{(2)_k \; k \; ! \; (2k+3)} \quad . \tag{55} $$

Hence,

$$ a_{k+1} = \frac{(-z^2/4)(k+3/2)}{(k+2)(k+1)(k+5/2)} \cdot a_k \tag{56} $$

is the recursion relation to be used for the series expansion, (54), when $abs(z) < 10$.

For abs(z) > 10, we need an asymptotic expansion for (54). Again, from [8, p. 199] we have

$$ {}_1F_2\left(\begin{matrix} 3/2 \\ 5/2, \quad 2 \end{matrix} \middle| \frac{-z^2}{4} \right) \sim \frac{6}{(2\pi)^{1/2}(z)^{5/2}} \cdot $$

$$ \cdot \left\{ e^{j(z-5\pi/4)} \cdot \Sigma \; (-j)^k \; d_k/z^k + e^{-j(z-5\pi/4)} \cdot \Sigma (j)^k \; d_k/z^k \right\} , \tag{57} $$

where the coefficients, $\{d_k\}$, satisfy the recursion relation

$$ d_0 = 1, \; d_1 = -7/8, \; 2(k+1)d_{k+1} = (3k^2 + 2k - 7/4)d_k - $$

$$ - (k + 3/2)(k - 1/2)(k - 3/2)d_{k-1} \; . \tag{58} $$

The final form of the asymptotic expansion is, therefore:

$$\int_0^z tJ_1(t)dt \sim 1 + \sqrt{\frac{z}{2\pi}} \left\{ e^{j(z-5\pi/4)} \Sigma\ (-j)^k\ d_k/z^k\ + \right.$$

$$\left. + e^{-j(z-5\pi/4)} \Sigma (j)^k\ d_k/z^k \right\} \quad . \tag{59}$$

The additional term of unity comes from the fact that

$$\int_0^z tJ_1(t)dt = - zJ_0(z) + \int_0^z J_0(t)dt$$

$$= - zJ_0(z) - \int_z^\infty J_0(t)dt + \int_0^\infty J_0(t)dt$$

$$= 1 - zJ_0(z) - \int_z^\infty J_0(t)dt \quad , \tag{60}$$

which agrees with (59).

(b) Numerical Evaluation of Infinite Integrals

The computation of the infinite integrals that appear in the matrix elements, (49), is performed by computing a sequence of partial sums of integrals over finite intervals and then applying the ε-algorithm in an attempt to accelerate the convergence of the sequence [9]. The finite integrals are computed by using a 30-point Gaussian quadrature; the length of the finite interval is determined empirically. The method has been used in other numerical electromagnetic codes [10].

V. RESULTS

After (47) is solved for the expansion coefficients, $\{b^{(r)}\}$, $\{b^{(z)}\}$, the results are then substituted into (37) to produce the components of

the induction field, $\bar{B}$, within the core. With this field in hand it is possible to compute other functions. In this section we illustrate some of the results that have been obtained for the E-shaped and cylindrical cores. Some of the results correspond to the workpiece being absent, in which case $\{b^{(r)}\}$ and $\{b^{(z)}\}$ are real. When the workpiece is present $\{b^{(r)}\}$ and $\{b^{(z)}\}$ are complex.

(a) Approximate $\bar{B}$-field Within the Core

Figure 7 shows the approximate $\bar{B}$-field within the cylindrical core, and Figure 8 shows the same thing for the E-shaped core, both when the workpiece is absent. In each case the line segments represent the approximate field at the center of each cell of the grid that was used in the method of moments. The line segments are shown emanating from the bottom or top line of a cell simply to facilitate the presentation.

The radius of the cylinder is 0.0625" and the height is 0.500". The inner radius of the coil is also 0.0625", the outer radius, 0.125", and the height is 0.250". The outer radius of the E-shaped core is 0.1875", and the height is 0.500". The same coil is used with the E-shaped core as with the cylinder. The permeability of the core is 1000 μ_0.

We note that $\bar{B}$ is generally smaller in magnitude for larger radii. This means that, because the cross-sectional areas increase with increasing radius, the net magnetic flux entering the region is equal to the net flux leaving, as is to be expected from the condition $\nabla \cdot \bar{B} = 0$. Indeed, we have computed an approximate value of $\nabla \cdot \bar{B}$ at one point within the cylindrical core and have found it to be zero, certainly within the accuracy of the expansion in pulse functions. This is a very desirable feature of our results; it shows that the model produces physically consistent and accurate results with the grids shown.

(b) Driving-point Impedance of the Coil and Core

The driving-point impedance of the coil is defined to be the ratio of the coil's induced voltage to its current. The voltage induced into a single turn of the coil located at (r',z') is given by

$$V(r',z') = -\oint \bar{E} \cdot d\bar{\ell} = j\omega 2\pi r' A(r',z') \quad , \tag{61}$$

which follows from the fundamental relation $\bar{E} = -j\omega\bar{A}$. The coil is uniformly and densely wound with n_c turns per unit area and occupies the rectangle $r_1 \le r \le r_2$, $z_1 \le z \le z_2$, as before. Hence, the net voltage induced into it is given by

$$V = j\omega 2\pi n_c \int_{r_1}^{r_2}\int_{z_1}^{z_2} rA(r,z)\,dr\,dz \quad . \tag{62}$$

The coil, of course, is in region 1, and the vector potential throughout region 1 is given by (13), which, after using (15) to transfer the curl to the Green's function and then substituting $\bar{M} = \bar{B}\,(\frac{1}{\mu_0} - \frac{1}{\mu})$, becomes

$$A(r,z) = 2\pi\mu_0 \iint_{coil} G_{11}(r,z;\, r',z')J(r',z')r'\,dr'\,dz'$$

$$+ 2\pi \iint_{core} (1 - \frac{\mu_0}{\mu})\bar{B}(r',z') \cdot \nabla' \times \bar{G}_{11}(r,z;\, r',z')r'\,dr'\,dz' \quad . \tag{63}$$

Thus, the induced voltage is given by substituting (63) into (62)

$$V = j\omega(2\pi)^2 n_c^2 I\mu_0 \int_{r_1}^{r_2} r\,dr \int_{z_1}^{z_2} dz \int_{r_1}^{r_2} r'\,dr' \int_{z_1}^{z_2} dz' G_{11}(r,z;\, r',z')$$

$$+ j\omega(2\pi)^2 n_c \int_{r_1}^{r_2} r\,dr \int_{z_1}^{z_2} dz \iint_{core} (1 - \frac{\mu_0}{\mu})\bar{B}(r',z') \cdot$$

$$\cdot \nabla' \times \bar{G}_{11}(r,z;\, r',z')r'\,dr'\,dz' \quad . \tag{64}$$

The first term on the right-hand side of (64) is the voltage that is induced into the coil in the absence of the core (the coil self-voltage), and the second term is the additional voltage induced into the coil due to the induced magnetization within the core. Upon using the expression for the Green's function, (34)(a), and then carrying out the integral in the first term of (64), the coil self-voltage becomes

$$j\omega 2\pi\mu_0 n_c^2 I \int_0^\infty \left[\frac{RF_1^2(z_1,z_2) + F_3(z_1,z_2,z_1,z_2)}{2\alpha_0}\right] \frac{I^2(r_1\ell, r_2\ell)}{\ell^3}\, d\ell\,, \quad (65)$$

where F_1, F_3, and I have been defined in (50).

The second term of (64) is evaluated after substituting (48) and (37), and then evaluating the integrals with respect to (r,z) and (r',z'). The result is

$$j\omega 2\pi(1 - \frac{\mu_0}{\mu})n_c \sum_{j=1}^{N_c} (b_j^{(r)}F_j^{(r)} + b_j^{(z)}F_j^{(z)})/\mu_0 n_c I, \quad (66)$$

where $F_j^{(r)}/\mu_0 n_c I$, $F_j^{(z)}/\mu_0 n_c I$ are the integral expressions of (49)(a),(b).

The total voltage induced into the coil is the sum of (65) and (66), and when this is divided by the coil current, I, the result is the driving-point impedance.

We have computed the driving-point impedance at four freuqencies, and present the results in Table 1. The columns in the table correspond to the dirving-point impedance of the coil alone, coil+cylindrical core, and coil+E-shaped core. The data are in ohms, and correspond to the dimensions stated in Subsection (a). The numbers in parentheses are powers of ten that multiply the adjacent number: for example, j0.2958(-2) = $j0.2958 \times 10^{-2}$. As a benchmark calculation to test the accuracy of our integration subroutine that uses the ε-algorithm (recall Section IV.(b)), we computed the inductance of the coil in air and compare it with the classical work of Grover [11]; the results are in excellent agreement. The inductance of the coil in air is determined from the first column in the upper-half of the table.

TABLE 1: DRIVING-POINT IMPEDANCE AT FOUR FREQUENCIES

AIR

COIL	CYLINDER	ESHAPE	FREQ
j0.2958(-2)	j0.1554(-1)	j0.3271(-1)	1kHz
j0.2958(-1)	j0.1554(-0)	j0.3271(-0)	10kHz
j0.2958(-0)	j0.1554(+1)	j0.3271(+1)	100kHz
j0.2958(+1)	j0.1554(+2)	j0.3271(+2)	1MHz

WORKPIECE

COIL X(-3)	CYLINDER X(-3)	ESHAPE X(-3)	FREQ
0.1075+j2.854	1.360+j13.84	1.401+j31.93	1kHz
1.284 +j26.37	10.77+j115.9	23.11+j279.9	10kHz
6.385 +j249.2	41.84+j1060.0	93.83+j2556.0	100kHz
23.14 +j2440.0	113.3+j10298.0	200.4+j24854.0	1MHz

BENCHMARK CALCULATION

INDUCTANCE OF COIL IN AIR

0.471 (-6) H (OUR MODEL)

0.473 (-6) H (GROVER, "INDUCTANCE CALCULATIONS," VAN NOSTRAND, 1946)

ALL CALCULATIONS ASSUME A CLOSE-PACKED COIL OF 20 GAUGE WIRE, CONSISTING OF 15.3 TURNS.

A more common presentation of the data in Table 1 is the impedance-plane plot of Figure 9. Here the real and imaginary parts of the driving-point impedance are displayed, with frequency as a parameter. The three curves correspond to the coil alone, coil+cylindrical core, and coil+E-shaped core, each in the presence of the workpiece. The interpretation of the diagram is that the coupling to the workpiece becomes tighter in going from the coil alone to the coil+E-shaped core.

The reactive part of the driving-point impedance is due partly to the self-inductance of the coil+core combination (as if the workpiece were absent) and partly to mutual interaction of the induced eddy-currents within the workpiece. The resistive part of the impedance is due entirely to the effects of the induced eddy-currents. At higher frequencies the eddy-currents reside nearer the surface of the workpiece, due to the skin-effect, therefore making the volume of interaction within the workpiece smaller. This means that the volume losses within the workpiece decrease, thereby decreasing the effective resistance of the workpiece, making the driving-point impedance of the coil+core combination reactive.

(c) Induced Fields Within the Workpiece

The purpose of the probe coil is to induce eddy-currents within the workpiece. It is a fairly straight-forward computation to determine the distribution of induced eddy-currents, once the induced magnetization within the core is known. The fundamental relation is

$$\bar{J}_2(r,z) = \sigma\bar{E}_2(r,z) = -j\omega\sigma\bar{A}_2(r,z) \quad , \tag{67}$$

where the subscript "2" denotes region 2, the workpiece, and σ is the conductivity of the workpiece. Hence, our first job is to determine an integral expression for $\bar{A}_2(r,z)$ in terms of the current and magnetization in region 1, where the coil and core are located. The details follow the method of Section II.

We start by replacing (6)(a),(b) by

$$\nabla \times \nabla \times \bar{G}_{12} - k_0^2 \bar{G}_{12} = 0 \qquad \begin{matrix}(r,z) \text{ in } 1 \\ (r',z') \text{ in } 2\end{matrix} \qquad (68)(a)$$

$$\nabla \times \nabla \times \bar{G}_{22} - k_1^2 \bar{G}_{22} = \frac{\delta(r-r')\delta(z-z')}{2\pi r'} \bar{a}_\phi \qquad \begin{matrix}(r,z) \text{ in } 2 \\ (r',z') \text{ in } 2\end{matrix} \qquad (b)$$

Next, we multiply (5) by the appropriate Green's function from (68) and then use the vector Green's identity over regions 1 and 2, as before, to get

$$2\pi\mu_0 \iint_{coil} J(r,z)G_{12}(r,z;\, r',z')\,rdrdz + 2\pi\mu_0 \iint_{core} \nabla \times \bar{M}(r,z) \cdot \bar{G}_{12}(r,z;\, r',z')\,rdrdz$$

$$= -2\pi \int_0^\infty [\bar{A}_1(r,z) \times \nabla \times \bar{G}_{12}(r,z;\, r',z') - \bar{G}_{12}(r,z;\, r',z') \times \nabla \times \bar{A}_1(r,z)]\Big|_{z=0} \cdot \bar{a}_z\, rdr \qquad (69)($$

$$A_2(r',z') = -2\pi \int_0^\infty [\bar{A}_2(r,z) \times \nabla \times \bar{G}_{22}(r,z;\, r',z') -$$

$$- \bar{G}_{22}(r,z;\, r',z') \times \nabla \times \bar{A}_2(r,z)]\Big|_{z=0} \cdot \bar{a}_z\, rdr \qquad (b)$$

which replace (8) and (9), respectively.

The boundary conditions on $\bar{G}_{12}$ and $\bar{G}_{22}$ at $z = 0$ are:

$$\bar{a}_z \times \bar{G}_{12} = \bar{a}_z \times \bar{G}_{22}$$

$$\frac{1}{\mu_1} \bar{a}_z \times \nabla \times \bar{G}_{22} = \frac{1}{\mu_0} \bar{a}_z \times \nabla \times \bar{G}_{12} \quad .$$

Arguing as before in Section II, we can show that the integral in (69)(b) is μ_1/μ_0 times the surface integral on the right-hand side of (69)(a). Therefore (69)(a) may be written

$$A_2(r',z') = 2\pi\mu_1 \iint_{coil} J(r,z)G_{12}(r,z;\ r',z')rdrdz$$

$$+ 2\pi\mu_1 \iint_{core} \nabla \times \bar{M}(r,z) \cdot \bar{G}_{12}(r,z;\ r',z')rdrdz \ . \quad (70)$$

There exists a reciprocity relation between $\bar{G}_{12}$ and $\bar{G}_{21}$:

$$\mu_1\bar{G}_{12}(r,z;\ r',z') = \mu_0\bar{G}_{21}(r,z;\ r',z') \ , \quad (71)$$

and with this (70) becomes

$$A_2(r',z') = 2\pi\mu_0 \iint_{coil} G_{21}(r',z';\ r,z)J(r,z)rdrdz$$

$$+ 2\pi\mu_0 \iint_{core} \nabla \times \bar{M}(r,z) \cdot \bar{G}_{21}(r',z';\ r,z)rdrdz \ . \quad (72)$$

This is the desired form because we have previously computed G_{21} in (34(b).

As usual, we transfer the curl operation to the Green's function in the second integral of (72) by using (15), and then we substitute $\bar{M} = \bar{B}(\frac{1}{\mu_0} - \frac{1}{\mu})$:

$$A_2(r',z') = \mu_0 n_c I \int_{r_1}^{r_2} rdr \int_{z_1}^{z_2} dz \int_0^\infty \frac{T}{\alpha_0} e^{(\alpha_1 z' - \alpha_0 z)} J_1(r\ell)J_1(r'\ell)\ell d\ell$$

$$+ \iint_{core} rdrdz(1 - \frac{\mu_0}{\mu})B_r(r,z) \int_0^\infty Te^{(\alpha_1 z' - \alpha_0 z)} J_1(r\ell)J_1(r'\ell)\ell d\ell$$

$$+ \iint_{core} rdrdz(1 - \frac{\mu_0}{\mu})B_z(r,z) \int_0^\infty Te^{(\alpha_1 z' - \alpha_0 z)} J_1(r'\ell)J_0(r\ell)\ell^2 d\ell \ . \quad (73)$$

When (37) is substituted into (73), and the integrals with respect to (r,z) and (r',z') are evaluated, we get the final expression

$$A_2(r',z') = \mu_0 n_c I \int_0^\infty \frac{T(\ell)}{\alpha_0} F_1(z_1,z_2) \frac{I(r_1\ell,r_2\ell)}{\ell} e^{\alpha_1 z'} J_1(r'\ell)d\ell$$

$$+ (1 - \frac{\mu_0}{\mu}) \sum_{j=1}^{N_c} (b_j^{(r)} C_j^{(r)} + b_j^{(z)} C_j^{(z)}) \qquad (74)$$

where

$$C_j^{(r)} = \frac{1}{r_b} \int_0^\infty T(\ell) F_1(z_j^{(-)},z_j^{(+)}) \frac{B_2(\ell r_j^{(-)},\ell r_j^{(+)})}{\ell^2} e^{\alpha_1 z'} J_1(r'\ell)d\ell \qquad (75)(a)$$

$$C_j^{(z)} = \int_0^\infty \frac{T(\ell)}{\alpha_0} F_1(z_j^{(-)},z_j^{(+)}) B_1(\ell r_j^{(-)},\ell r_j^{(+)}) e^{\alpha_1 z'} J_1(r'\ell)d\ell \quad . \qquad (b)$$

Using (74) we have computed the induced $\bar{E}$-field in air, and the induced eddy-currents in the workpiece, as a function of radial position at two depths, z = 0 and z = -2.7mm, as shown in Figure 10. The latter depth is the skin-depth in aluminum ($\sigma = 3.5 \times 10^7$) at 1kHz.

In Figure 11 we show $\bar{E}$ in air at these two depths, the three curves corresponding to the three core/coil combinations, coil alone, coil+cylinder, and coil+E-shape. The reduction in field intensity at -2.7mm is not due to skin effect (the workpiece is absent), but is simply due to distance; this is a manifestation of "lift-off." It is clear from part (a) of the figure that the coil alone produces the weakest field and that the E-shaped core produces the strongest peak. This is to be expected. A more interesting result, however, is that the E-shaped field falls off very quickly, and becomes the weakest of the three fields beyond the radial limit of the core. This is due to the fact that the net magnetic flux that is linked by a circular path beyond this radius is practically zero, because virtually all of the flux leaving the outer leg

returns through the middle leg. Hence, we conclude that the E-shaped core is effective for producing an intense, concentrated field. The results of Figure 11 are independent of frequency over the range 1kHz to 1MHz.

The presence of the workpiece enhances the concentrating effect of the coil/core combinations, as Figure 12 shows. Here, the induced eddy-currents are shown at 1kHz. The fields now are complex, so that the real and imaginary parts are both shown, the imaginary part dominating. If the curves of Figure 11 are compared with the curves of the imaginary parts (marked "I") of Figure 12, it will be seen that the latter curves fall off more rapidly with r, for all three combinations of coil and core. This enhanced concentration is due to Lenz' law, which states that induced currents flow in such a direction as to oppose the flux that produces them. If the flux is reduced then the electric field and eddy-currents must fall off more rapidly with radial distance. The reduction of the fields at -2.7mm, as shown in part (b) of the figure, is now principally due to skin effect.

The effects of increasing frequency are shown in Figure 13, which illustrates the real and imaginary parts of the induced eddy-currents at 1MHz. At this frequency these parts are approximately equal, and the fields vanish, due to skin-effect, at -2.7mm (which, it will be recalled, is the skin-depth at 1kHz). The rather erratic nature of the curves that correspond to the coil+cylinder and coil+E-shape combinations is probably due to numerical instabilities in computing the coefficient integrals $C_j^{(r)}$ and $C_j^{(z)}$ of (75). We are presently investigating methods for smoothing these data.

In all of the cases that are illustrated in Figures 11-13, it is clear that the E-shaped core is most effective in coupling energy into the workpiece, as was first suggested in the discussion of Figure 9. This is another indication of the internal consistency of our model.

VI. COMMENTS, EXTENSIONS AND CONCLUSIONS

Our objective in this report was to apply modern methods of computational electromagnetics to develop a model of eddy-current probe coils with ferrite cores, which would provide a systematic and rational basis for the design and characterization of such coils. The model that we have demonstrated meets this goal; in addition, it is physically and mathematically consistent.

Our approach was to use a volume integral equation and the method of moments. Other approaches are available, namely finite elements, and a surface integral equation plus the method of moments. The volume integral equation approach resulted in a simpler model, that required only a single Green's function (for the whole of regions 1 and 2), rather than a Green's function for the interior of the ferrite core and a separate Green's function for the exterior, as would have been required in the other two approaches. This resulted in simpler programming for the computer. It is usually true, however, that different problems favor different methods, and one must be familiar with all approaches in order to select the one that is most efficient.

The model that we have derived is useful for the analysis of probes with linear, isotropic ferrite cores. It can be extended to apply to the following problem areas, all of which are important in contemporary eddy-current NDE technology:

- Analyze probe coils with anisotropic (single crystal) cores
- Time-dependent (pulsed) eddy-current problems (linear core)
- Time-dependent (pulsed) eddy-current problems (nonlinear core)
- Optimization of probe coil design to satisfy simultaneous constraints on eddy-current distribution and driving-point impedance

In principle, the only extension that is required of the present model in order to treat the first and third problems is to define a

different $\bar{B}$ vs. $\bar{M}$ relationship than the one used here. For the single crystal problem this relationship would remain linear, but would involve a tensor permeability, rather than the scalar μ.

The nonlinear problem probably can be approached through the theory of micromagnetics [12], which would require the simultaneous solution of a volume integral equation of the type described in this report and a nonlinear partial differential equation (the fundamental equation of micromagnetics). It is possible that the best approach to the numerical computation with such a model would be a combination of finite elements and the method of moments.

All of these problems are solvable; they only require a sustained modeling effort. The rewards for such an effort could be immense in terms of improved design and understanding of probe coils with ferrite cores.

VII. REFERENCES

[1] C. V. Dodd and W. E. Deeds, "Analytical Solutions to Eddy-Current Probe-Coil Problems," J. Appl. Phys., 39, 2829-2838 (1968).

[2] J. W. Luquire, W. E. Deeds, and C. V. Dodd, "Alternating Current Distribution Between Planar Conductors," J. Appl. Phys., 41, 3983-3991 (1970).

[3] C. C. Cheng, C. V. Dodd, and W. E. Deeds, "General Analysis of Probe Coils Near Stratified Conductors," Intern. J. Nondestructive Testing, 3, 109-130 (1971).

[4] R. Mittra, ed., Computer Techniques for Electromagnetics, New York, Pergamon Press, 1973.

[5] R. Mittra, ed., Numerical and Asymptotic Techniques in Electromagnetics, New York, Springer-Verlag, 1975.

[6] Roger F. Harrington, Field Computation by Moment Methods, New York, The Macmillan Company, 1968.

[7] M. Abramowitz and I. A. Stegun, eds., Handbook of Mathematical Functions, Washington D.C., Nat. Bur. Standards, 1970.

[8] Y. L. Luke, The Special Functions and Their Approximations, New York, Academic Press, 1969.

[9] Jet Wimp, Sequence Transformations and Their Applications, Ch. 6, New York, Academic Press, 1981.

[10] D. L. Lager and R. J. Lytle, "Fortran Subroutines for the Numerical Evaluation of Sommerfeld Integrals Unter Anderem," Lawrence Livermore Laboratory, May 21, 1975.

[11] Frederick W. Grover, Inductance Calculations, New York, D. Van Nostrand, 1946.

[12] William Fuller Brown, Jr., Micromagnetics, New York, Interscience Publishers, 1963.

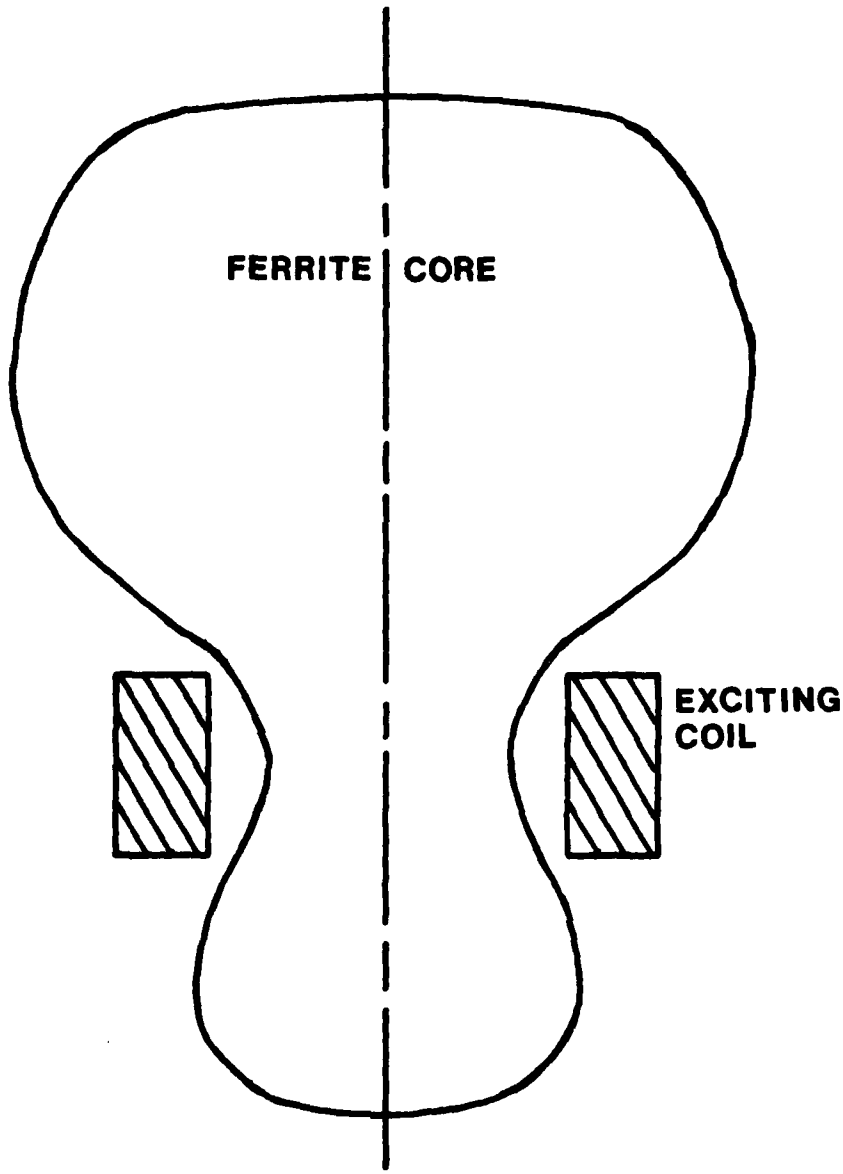

Figure 1. Ferrite core in the shape of a general body-of-revolution, with its exciting coil, in the presence of a stratified half-space workpiece.

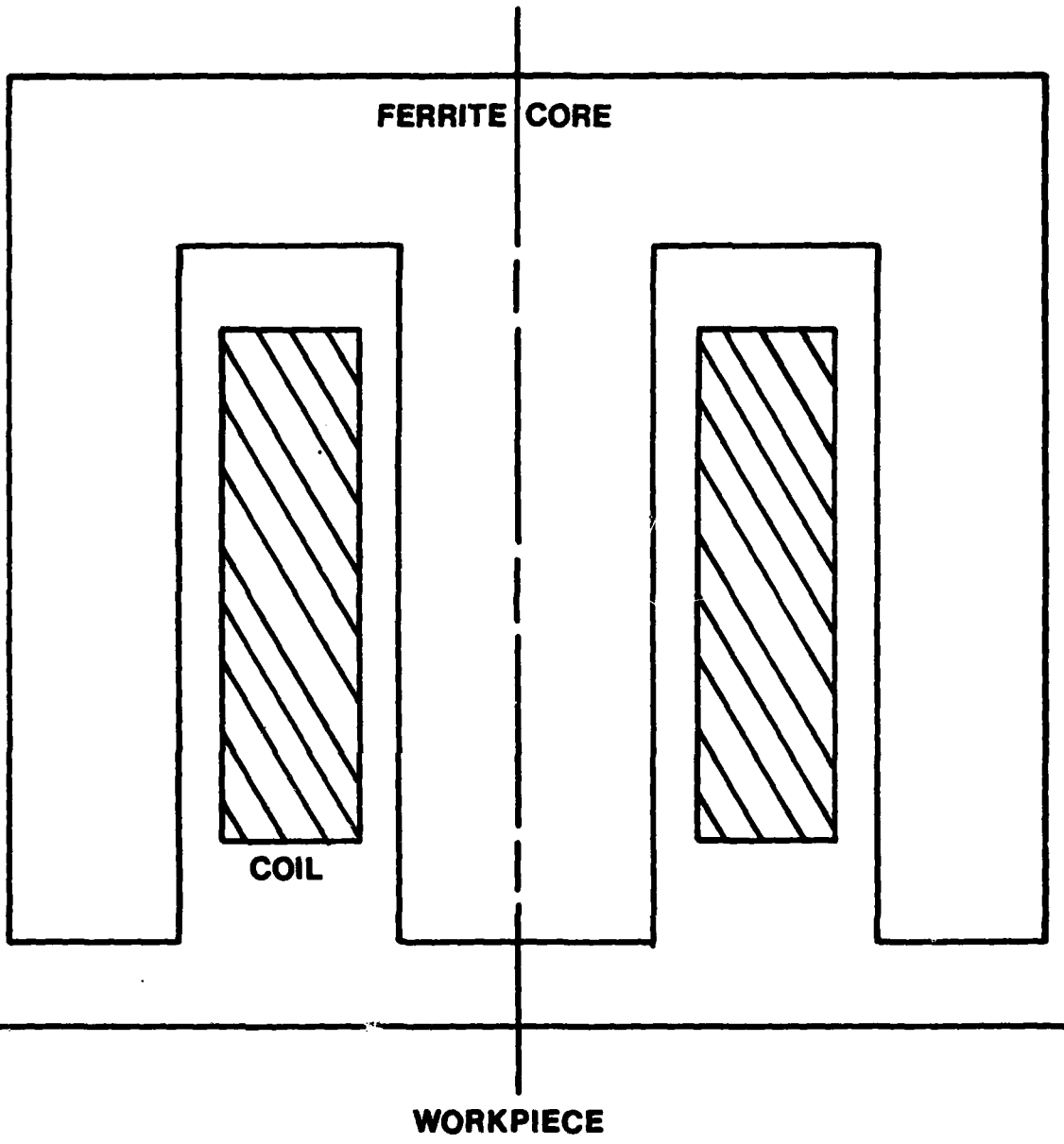

Figure 2. E-shaped body-of-revolution with exciting coil.

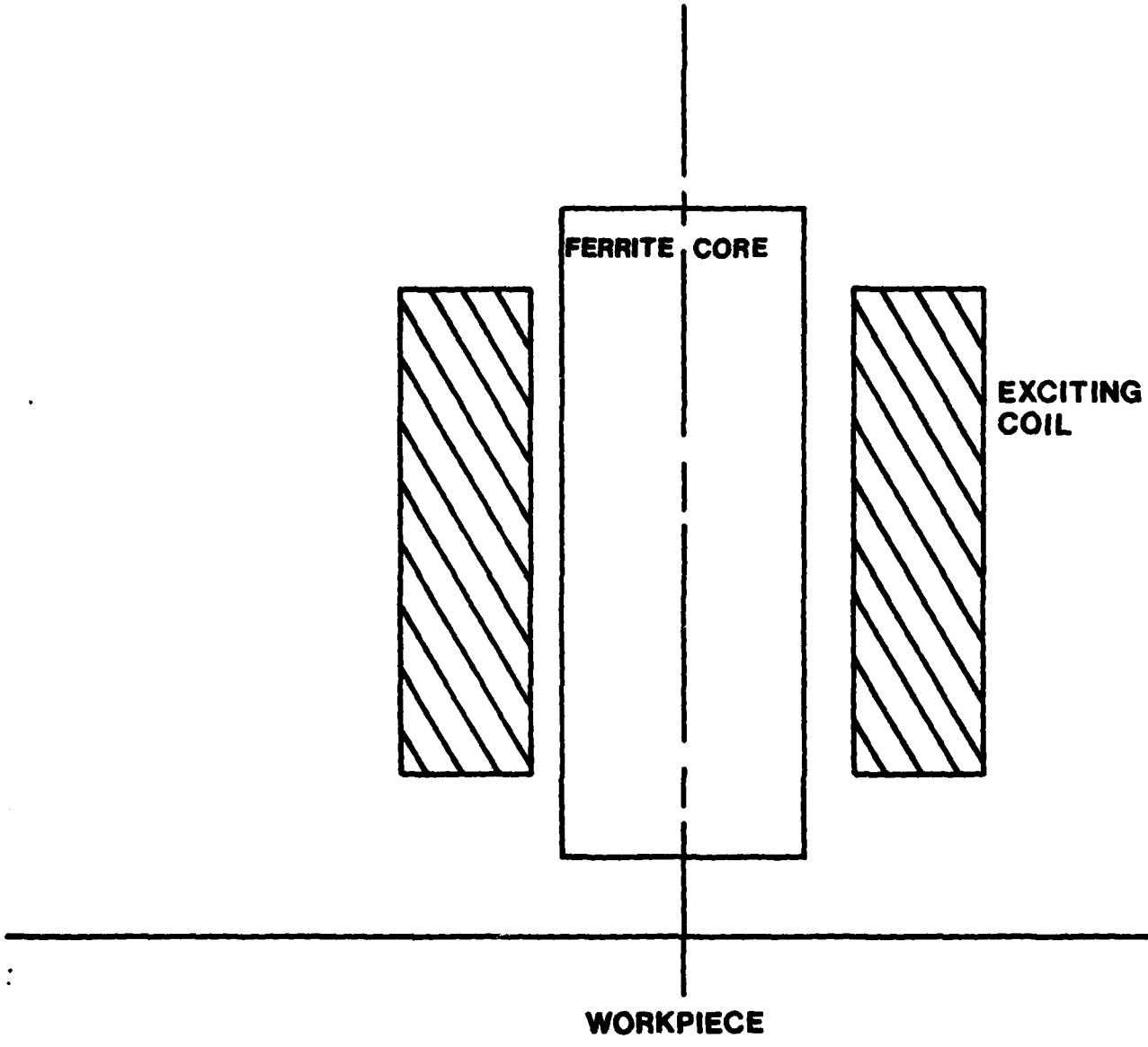

Figure 3. Truncated cylinder with exciting coil.

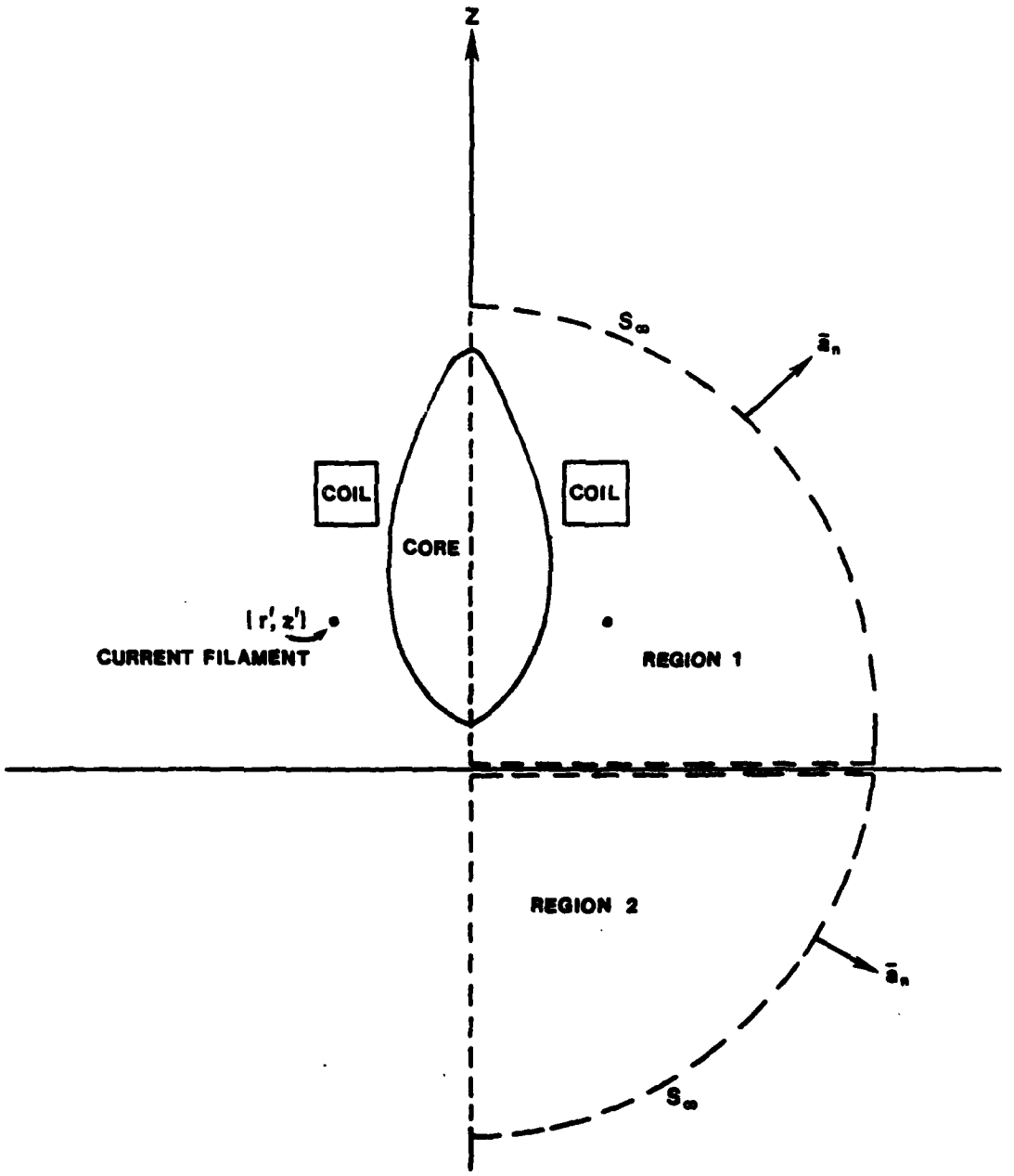

Figure 4. Showing the two regions and surfaces that are used in the application of the vector Green's identity to the derivation of the volume integral equation.

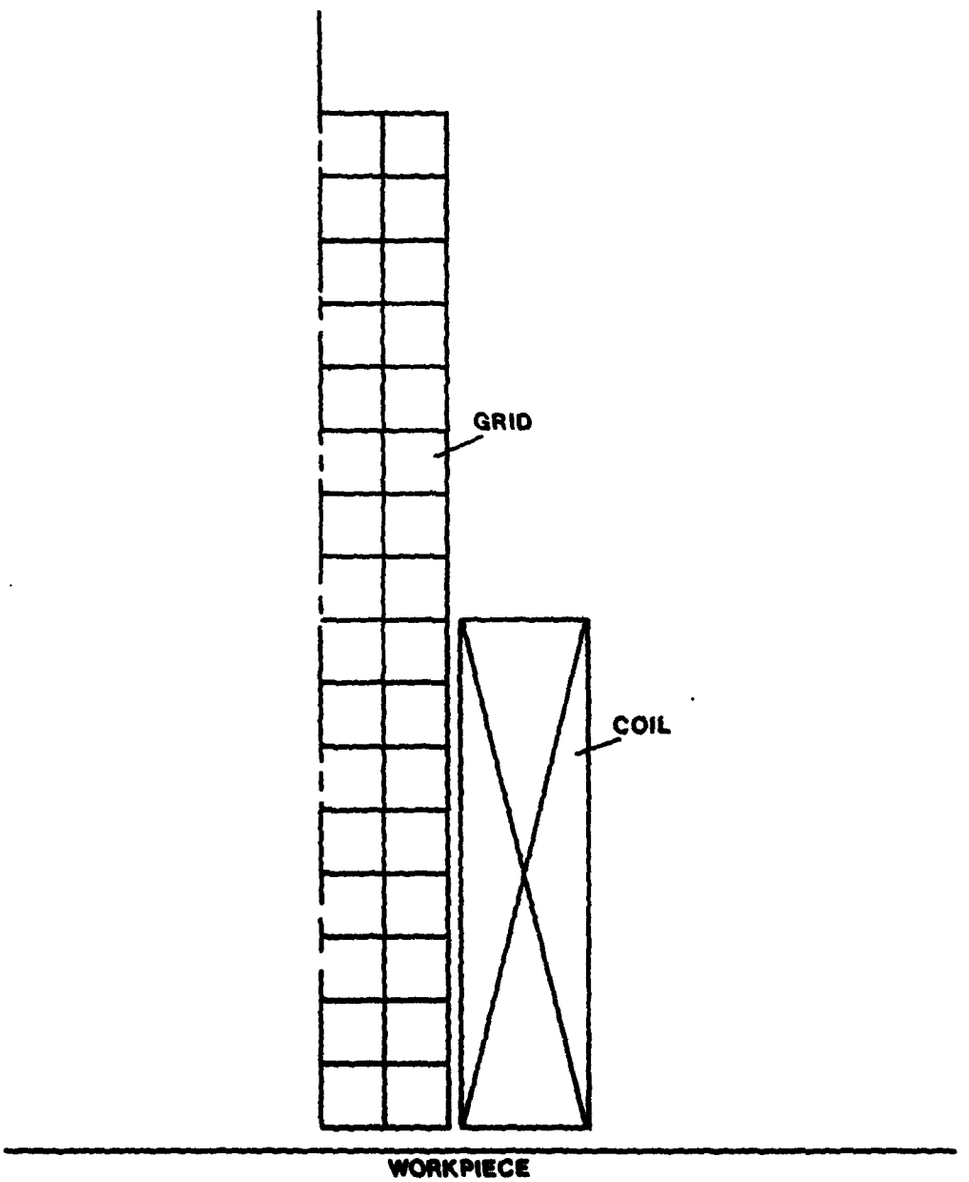

Figure 5. A partitioning of the cylindrical core into a regular grid, for applying the method of moments.

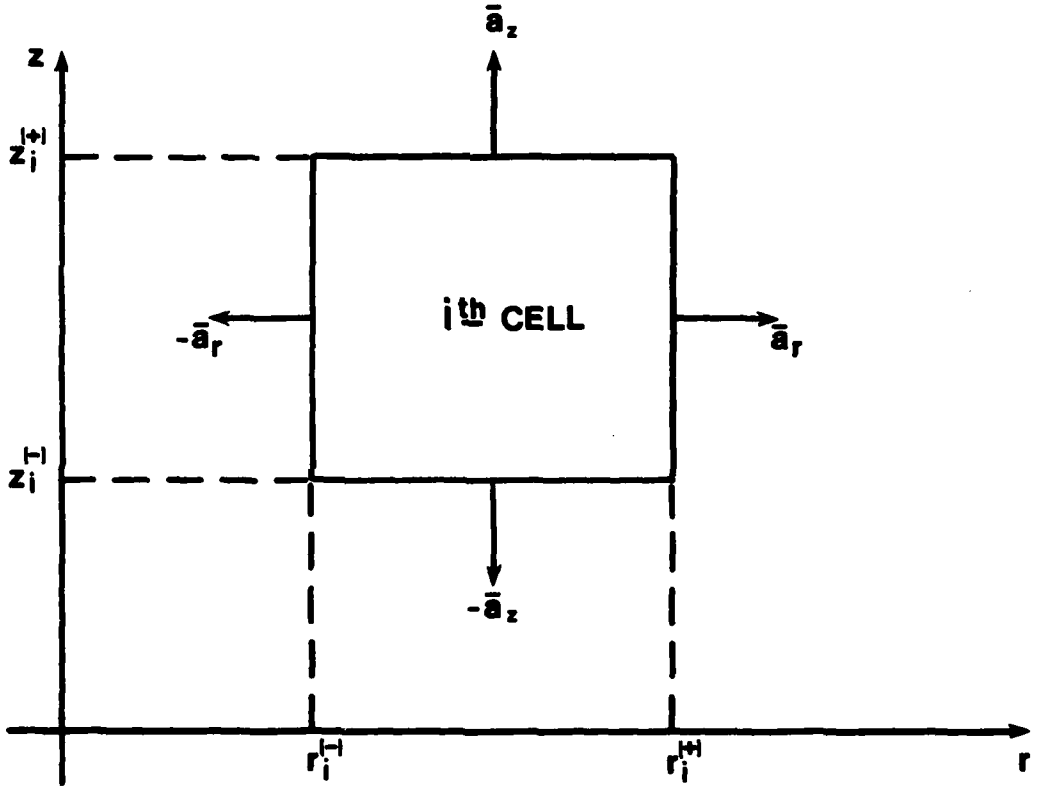

Figure 6. Definition of ith cell boundaries, for computation of integrals.

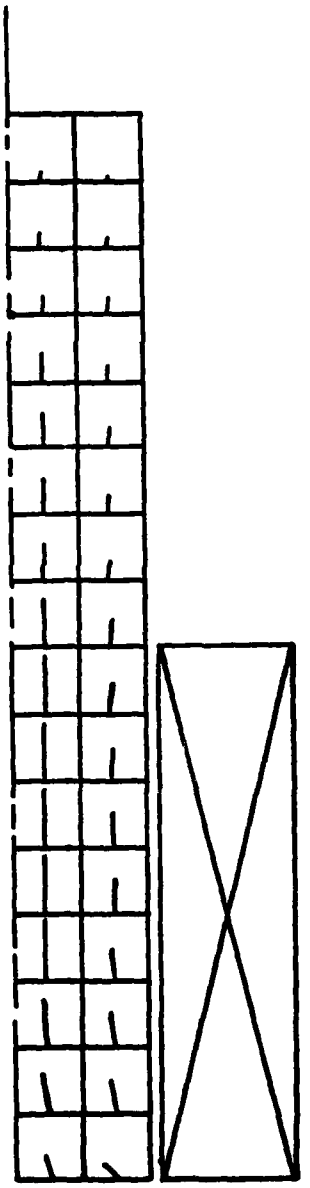

Figure 7. Approximate $\bar{B}$-field within the cylindrical core.

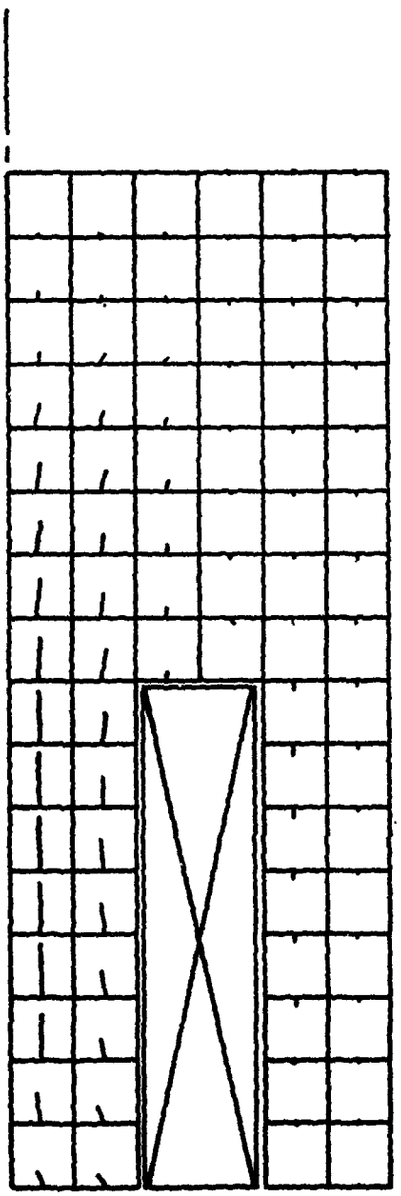

Figure 8. Approximate $\tilde{B}$-field within the E-shaped core.

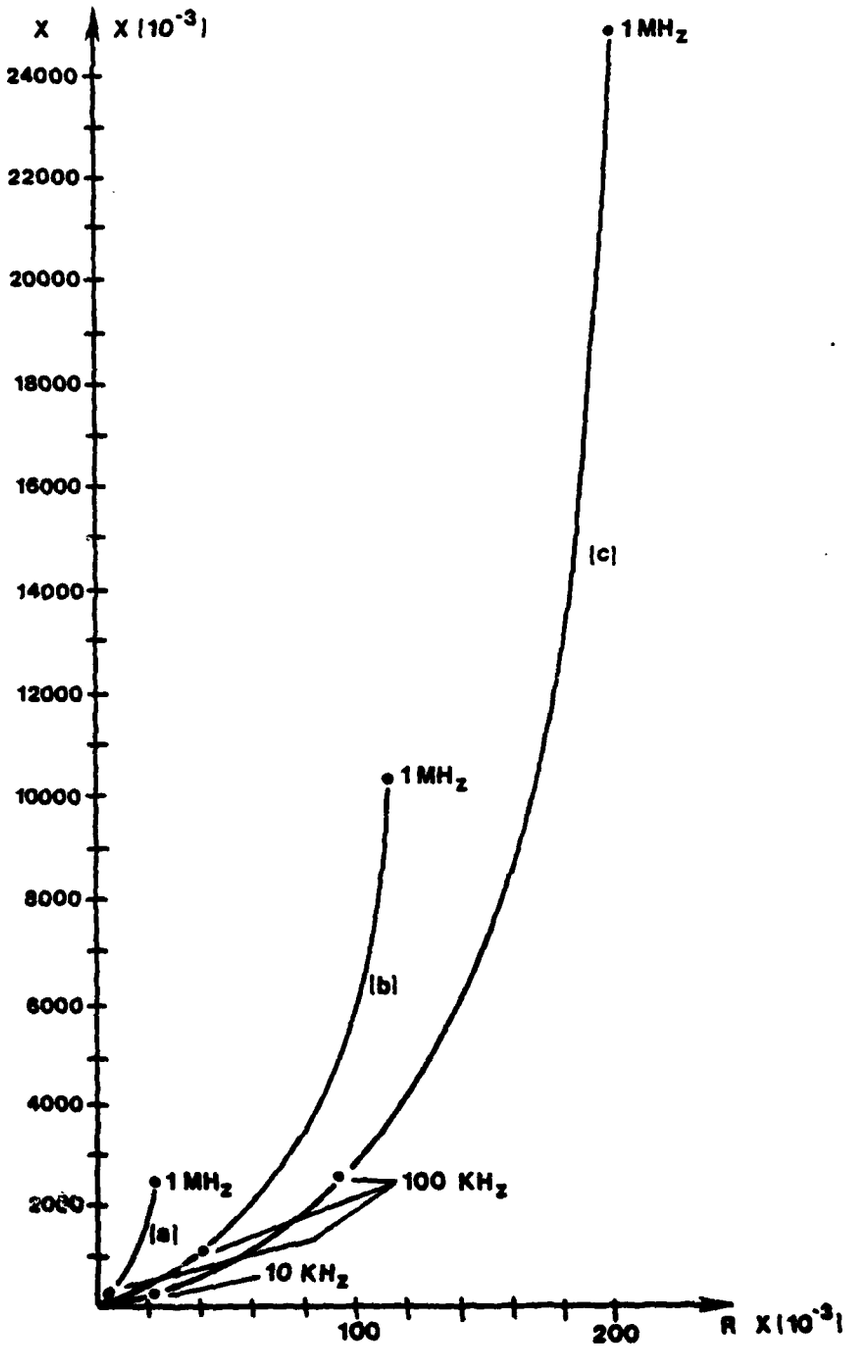

Figure 9. Impedance-plane plot of driving-point impedance. (a) coil alone, (b) coil+cylindrical core, (c) coil+E-shaped core.

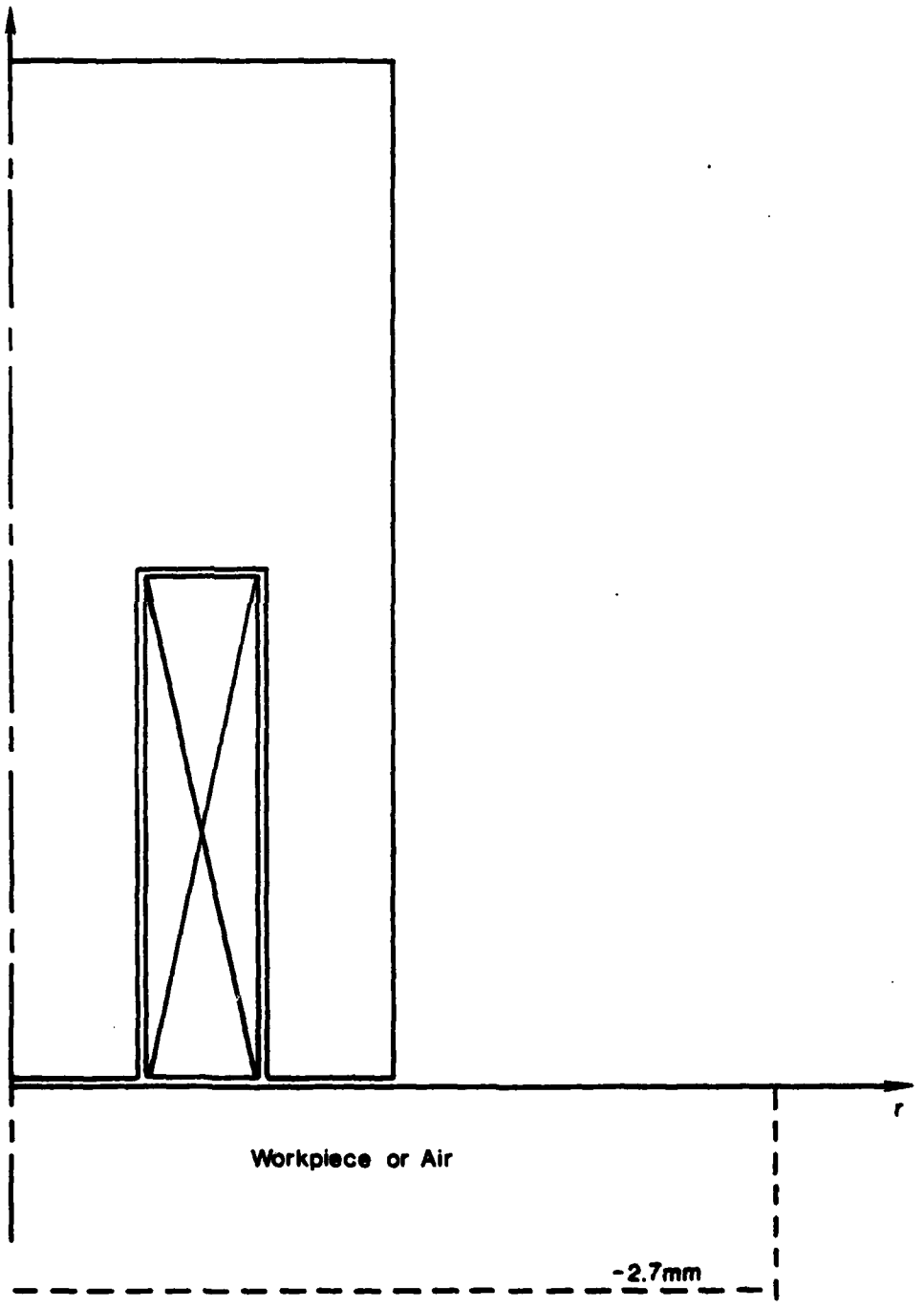

Figure 10. Showing coil+core and region of workpiece, or air, in which eddy-currents, or E-field, are calculated.

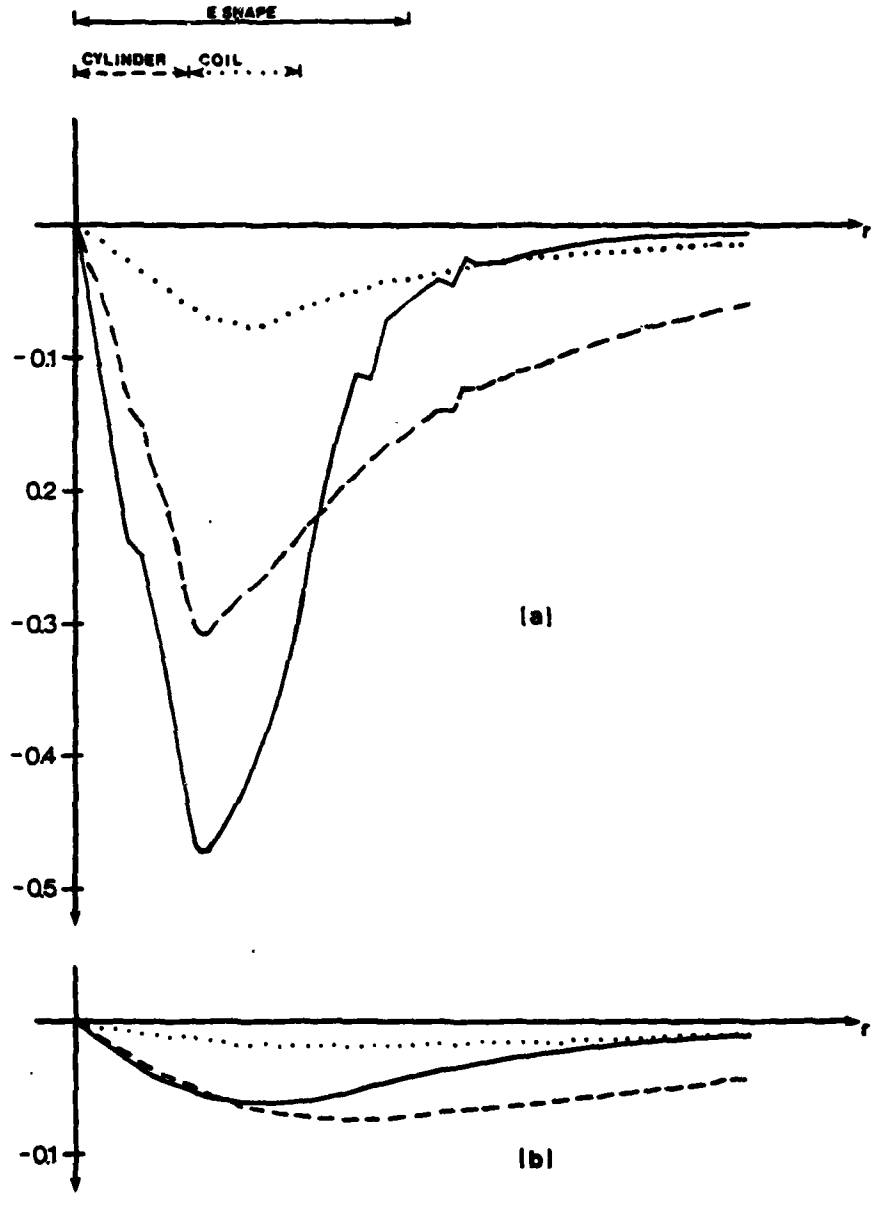

Figure 11. E-field in air at surface, (a), and -2.7mm, (b), levels of region of Figure 10.

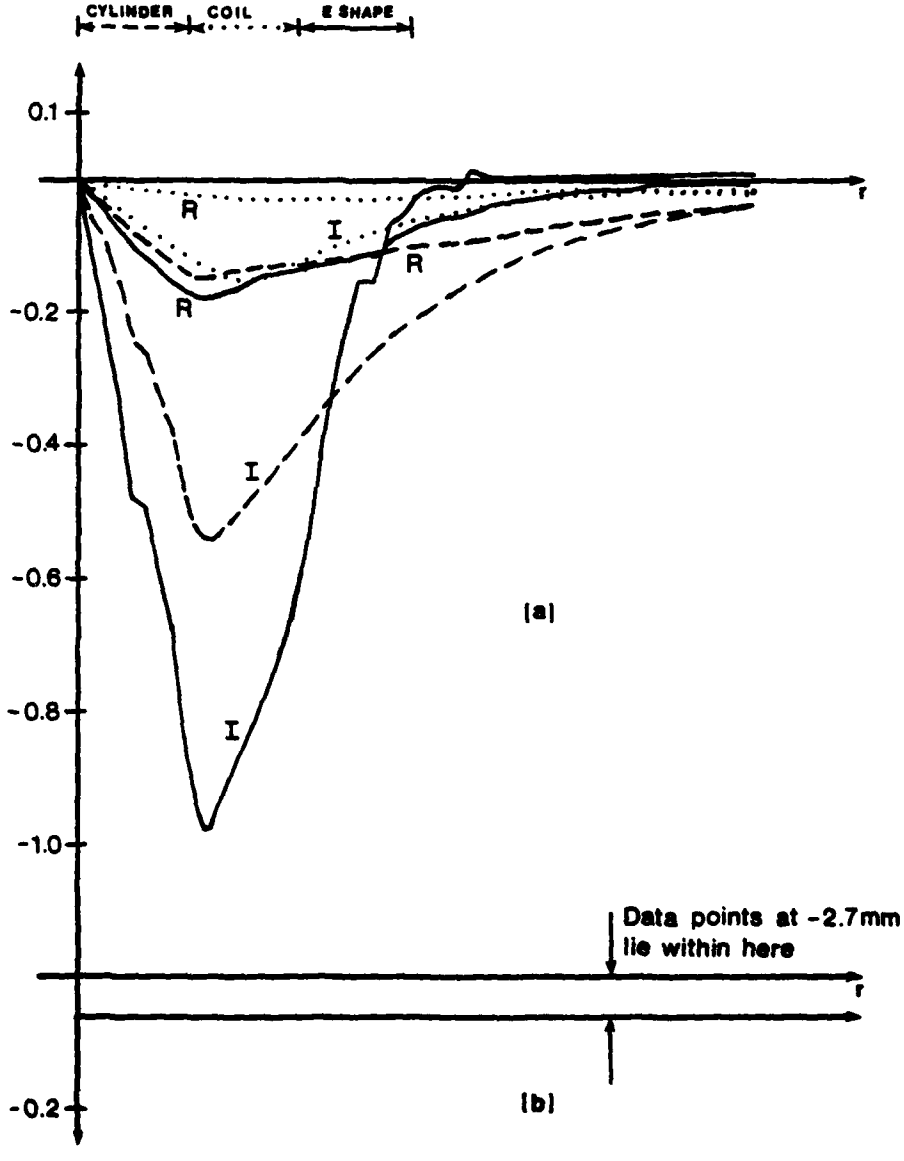

Figure 12. Induced eddy-currents in workpiece, at 1 kHz. (a) surface, (b) -2.7mm. R=real part, I=imaginary part. Upper-left legend indicates radial extent of core-shapes and coil.

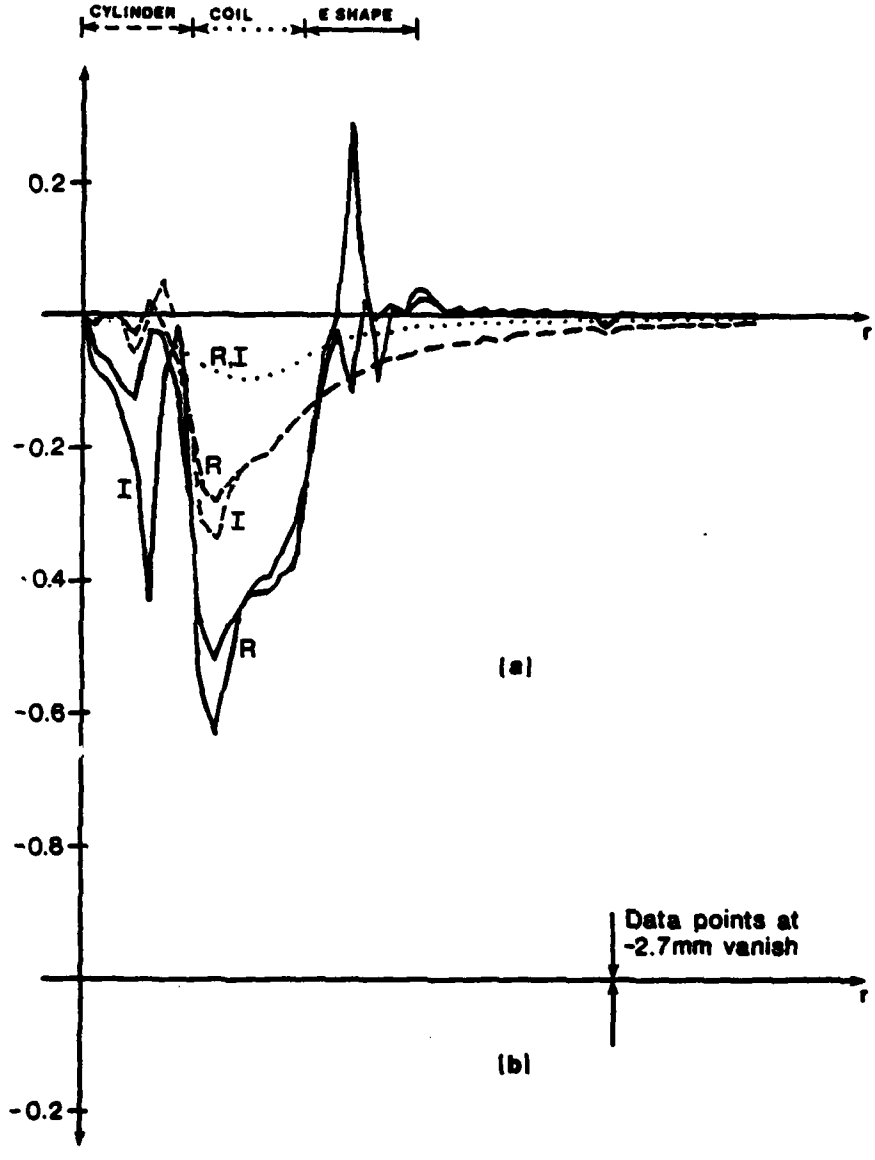

Figure 13. Induced eddy-currents in workpiece, at 1 MHz. (a) surface, (b) -2.7mm. R=real part, I=imaginary part. Upper-left legend indicates radial extent of core-shapes and coil.

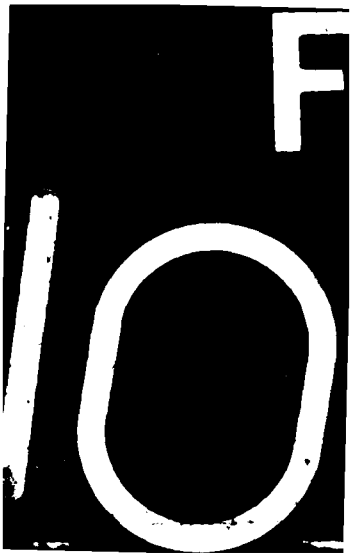
F
10